

1 **Electrochemical membrane reactors for the utilisation of** 2 **carbon dioxide**

3
4 Ivan Merino-Garcia^a, Enrique Alvarez-Guerra^a, Jonathan Albo^b, Angel Irabien^{a*}

5
6 *^aDepartment of Chemical and Biomolecular Engineering, University of Cantabria, Avenida de
7 los Castros s/n, 39005 Santander, Cantabria, Spain.*

8 *^bDepartment of Chemical Engineering, University of the Basque Country, Apdo. 644, 48080,
9 Bilbao, Spain.*

10 *Corresponding author; e-mail: angel.irabien@unican.es

11
12 Climate Change is among the greatest challenges for humankind in the 21st century.

13 Carbon Capture and Utilisation (CCU) allows the production of value-added chemicals
14 from CO₂, reducing at the same time the undesirable effects of global warming.

15 Among the available methods for CO₂ utilisation, the electrochemical reduction appears
16 as a promising technological solution to store intermittent renewable energy in the form
17 of chemical bonds, leading to valuable chemicals such as formic acid, methanol or
18 ethane, which can be put back into the market.

19 The application of electrochemical membrane reactors (ecMRs) for the valorisation of
20 CO₂ allows the separation of the catholyte and anolyte compartments, leading to an
21 enhanced separation of reaction products and avoiding their re-oxidation. Among these
22 membrane-based reactors, the utilisation of Membrane Electrode Assemblies (MEAs),
23 where the cathode and anode are coupled with a conductive membrane, are gaining
24 importance. Besides, Gas Diffusion Electrodes (GDEs) are able to reduce mass transfer
25 limitations and therefore, enhanced efficiencies in the process of CO₂ electroreduction.

26 Accordingly, the aim of the present review is to compile the literature on the application
27 of membrane reactors for CO₂ electroreduction, paying special attention to the type of
28 membrane, reactor configuration and catalytic material in the electrochemical reactor.

29 Then, a performance comparison in terms of Faradaic efficiency and products reported
30 up to date, is carried out.

31

32 **1. Introduction**

33 Climate change is one of the most significant challenges to achieving sustainable
34 development. The emissions of carbon dioxide (CO₂) to the atmosphere need therefore
35 to be drastically reduced in order to alleviate the proven effects of global warming [1,
36 2].

37 Among the available CO₂ mitigation strategies, Carbon Capture and Utilisation (CCU)
38 to produce useful chemicals from CO₂ [3-5] is particularly interesting, since it may
39 alleviate our rely on fossil fuels for energy and chemical synthesis [6], promoting, at the
40 same time, new technical sinks in the carbon life cycle.

41 There are different techniques to activate and convert CO₂ at low temperatures. Among
42 them, photoreduction (photocatalysis), electrochemical reduction (electrocatalysis) and
43 reforming of CO₂ are considered the most interesting ones [7].

44 The technology for CO₂ photoreduction is still incipient. Photocatalytic materials seem
45 to be unstable and current efficiencies are still low. Besides, plasma methods are clean
46 and fast, but their energy efficiency is still very low (around 6 %). On the other hand,
47 conventional methods (i.e. reforming) involve high cost associated to the needs of high
48 thermal power [7].

49 In contrast, the electrocatalytic reduction of CO₂ is an attractive solution since it allows
50 obtaining hydrocarbons and oxygenates with a simple procedure at low operation
51 temperatures. In addition, this technique shows promise to reduce greenhouse gas

52 emissions and control the anthropogenic carbon cycle by transforming CO₂ to fuels and
53 chemicals [8]. Due to the environmental and potential economic benefits, different
54 systems have been developed for the electrochemical conversion of CO₂ [9].

55 The efficiency of this process can be enhanced by selecting a highly active
56 electrocatalytic material, increasing the pressure of CO₂ (using gas diffusion electrodes
57 (GDEs)) or applying efficient electrochemical reactor configurations, among others
58 [10].

59 Besides, the application of membranes in electrochemical reactors for CO₂ reduction is
60 also interesting, since it allows separating the cathodic and anodic reactions that occur
61 simultaneously in a redox system. Thus, studies on CO₂ conversion in divided
62 electrochemical membrane reactors (ecMRs) are commonly found in literature [11].

63 Membranes may play a very important role, since they allow the use of different
64 catholyte and anolyte volumes, enhancing the separation of products, leading to
65 technical advantages in the reduction process. Besides, Membrane Electrode
66 Assemblies (MEAs), where cathode and anode are coupled with conductive membrane
67 materials, are also an interesting approach. The literature shows the application of
68 different ion exchange membranes for the electrochemical reduction of CO₂ in divided
69 cells, namely cation exchange membranes (CEMs), usually Nafion[®], and anion
70 exchange membranes (AEMs) such as Selemion[™]. In addition, the phase involved in
71 these reactors has also been taken into account. Works based on gas phase at the
72 cathode side are emerging due to the low solubility of CO₂ in water [12], with the aim
73 to improve mass transfer limitations occurring in liquid phase systems. Moreover, the
74 utilisation of gas phase in both, the cathode and anode compartments, has been reported
75 in a few works [13, 14], although the efficiencies of those systems are still low, and
76 therefore, further developments are needed.

77 There are several reviews on different aspects related to CO₂ electrochemical
78 conversion [6, 9, 15-17]. However, none of them pays specific interest to the discussion
79 on membrane reactor configurations for CO₂ electroreduction. Thus, the aim of the
80 present review is to discuss the different reports on electrochemical membrane reactor
81 configurations for CO₂ utilisation. A discussion of relevant studies on the topic are
82 presented, emphasizing on: membrane materials, electrochemical reactor designs and
83 catalytic material for each system.

84

85 **2. Electrocatalytic reaction analysis**

86 The performance of a CO₂ electrochemical reduction process is in general evaluated in
87 terms of *Faradaic efficiency (FE)*, *energy efficiency (EE)* and *current density (CD)*. The
88 *FE* represents the percentage of electrons that end up in the desired product:

$$89 \quad FE (\%) = \frac{z \cdot n \cdot F}{Q} \times 100 \quad (1)$$

90 where z is the number of exchanged electrons, n is the number of moles for a product, F
91 is the Faraday constant (96,485 C·mol⁻¹), and Q represents the charge passed in the
92 system (C).

93 Besides, the *energy efficiency (EE)* refers to the amount of energy in the products
94 divided by the amount of electrical energy put into the system [8], as defined by
95 equation 2:

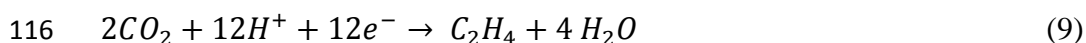
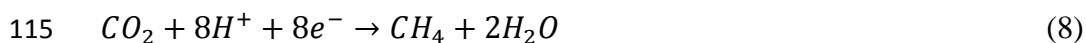
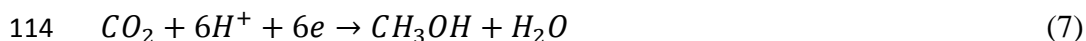
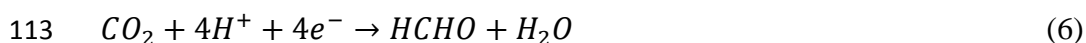
$$96 \quad EE = \sum_k \frac{E_k^0 \cdot FE_k}{E_k^0 + \eta} \quad (\text{dimensionless}) \quad (2)$$

97 where E_k^0 is the equilibrium cell potential for a specific product k (V), FE_k is the *FE* of
98 product k , and η is the cell overpotential (V) [6].

99 And finally, the *current density (CD)*, which is related to the conversion rate of the
100 electrochemical reaction, usually expressed in mA·cm⁻².

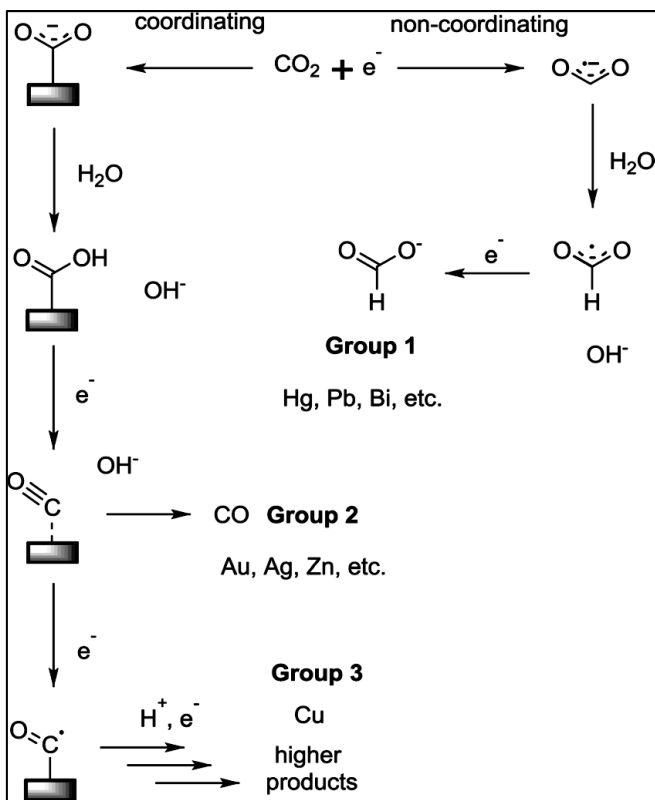
101 The goal for an efficient CO₂ electroreduction process is to achieve high *EEs* and
102 reaction rates for CO₂ conversion (i.e., high *CD*). Therefore, high *FE* and low
103 overpotentials on the cathode and anode are necessary in order to bring the technology
104 closer to an industrial scale.

105 Moreover, the reduction products obtained from the electroreduction of CO₂ are diverse,
106 mainly including carbon monoxide (CO), formic acid (HCOOH), formaldehyde
107 (CH₂O), methanol (CH₃OH), methane (CH₄), ethylene (C₂H₄) or ethanol (CH₃CH₂OH),
108 depending on the number of electrons involved as shown from equation 3 to equation 9.
109 It is also very common to find a mixture of products [6, 16, 18].



117 The mechanisms for CO₂ reduction on metallic electrodes have been hypothesized by
118 several authors, as summarized in Figure 1 [6, 8, 16].

119 In general, metal groups 1 and 2, which lead to CO and HCOOH formation, are widely
120 found in the literature [19, 20]. On the other hand, studies applying metals included in
121 the group 3 for alcohols and hydrocarbon formation are less abundant [21, 22].



122

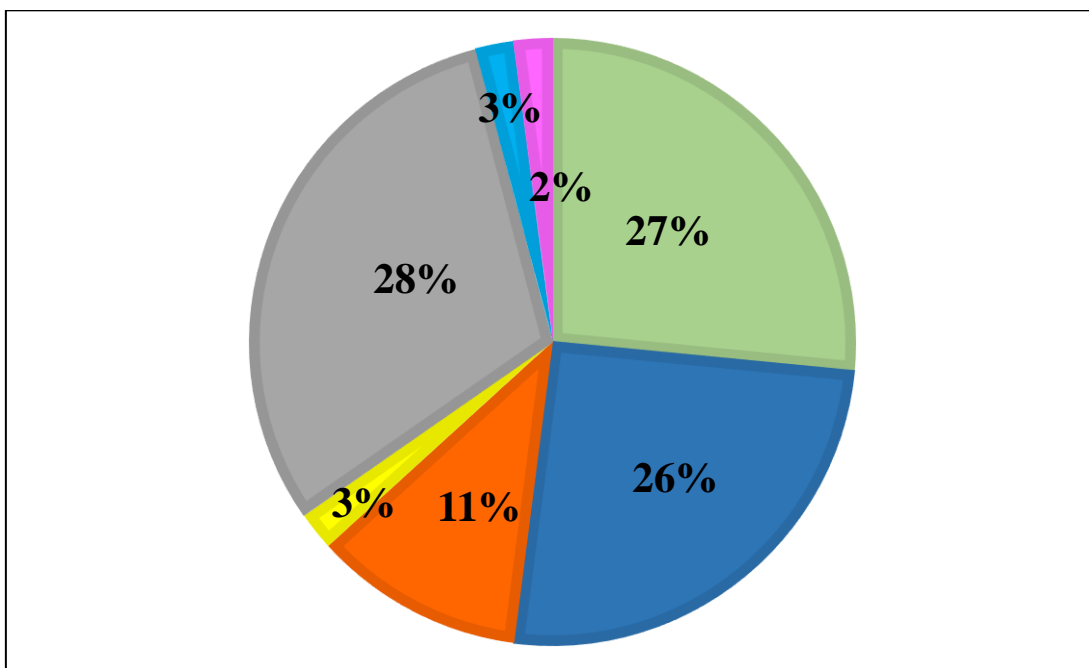
123 Figure 1. Mechanisms for the electrochemical reduction of CO₂ in water at metal

124 surfaces. Reproduced with permission from ref. [8].

125

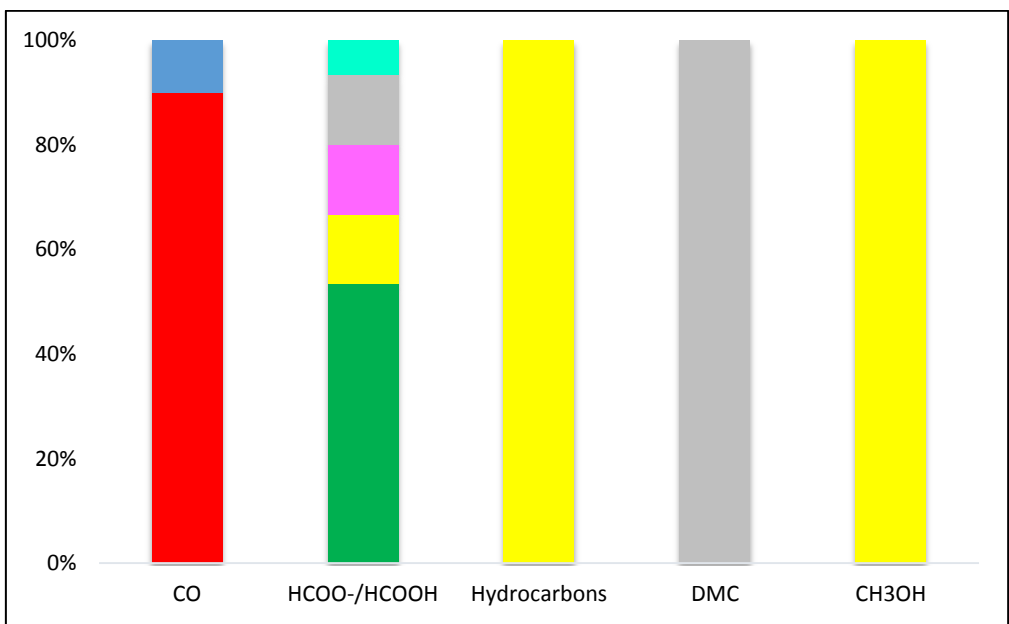
126 In order to give an overview of the available literature in the valorisation of CO₂ using

127 ecMRs, Figure 2 shows the products distribution of reported systems.



128

129 Figure 2. Distribution products, reports for CO₂ utilisation in ecMRs. Notation:
 130 HCOOH; CO; CH₄; C₂H₄; C₂H₆; CH₃OH; dimethyl carbonate (DMC)
 131 [revised March 2016].
 132
 133 HCOOH and CO are the main products in ecMRs, due to their lower number of
 134 electrons and protons exchanged. Besides, the production of hydrocarbons (i.e. CH₄,
 135 C₂H₄ and C₂H₆) are gaining increasing importance, in spite of the higher number of
 136 electrons and protons required in the process [9, 15]. On the other hand, CH₃OH (3 %) and
 137 DMC (2 %) have been scarcely found to be the main products in ecMR systems.
 138 Considering the relevance of the cathode material in the CO₂ electroreduction process,
 139 Figure 3 shows the type of catalysts applied for the production of different products in
 140 ecMR systems.



141
 142 Figure 3. Different catalysts applied for the formation of different products obtained.
 143 Notation: Ag; Ni; Sn; Pb; Pt; Cu; Cu-Sn
 144 As observed, CO is generally obtained in ecMRs with Ag-based catalysts (90 %).
 145 Besides, Sn-based catalysts are the most common reported materials for HCOOH

146 production, although Pb, Pt, and Cu-based catalysts can be also active for HCOOH
147 formation in ecMRs [20, 23-25]. Cu-based catalyst have been mainly used for the
148 electrochemical conversion of CO₂ to hydrocarbons and CH₃OH [21, 26]. DMC has
149 been obtained at Pt-Nb catalysts (95 % Pt). The figure, thus, demonstrates the
150 importance of the cathodic material selection in the valorisation of CO₂, in order to
151 achieve high efficiencies for different products.

152 Some electrocatalysts for the electrochemical reduction of CO₂ gave desirable product
153 selectivity under continuous operation, but only a few of them have resulted in high
154 efficiency production (e.g. Sn and Pb to obtain HCOOH). In this way, the selectivity to
155 the desired product with high efficiencies strongly depends on other aspects related to
156 the process such as the composition of electrocatalysts, the catalytic mechanism for CO₂
157 reduction or operation conditions (pH, electrolyte, potential, temperature, pressure, etc.)
158 [18].

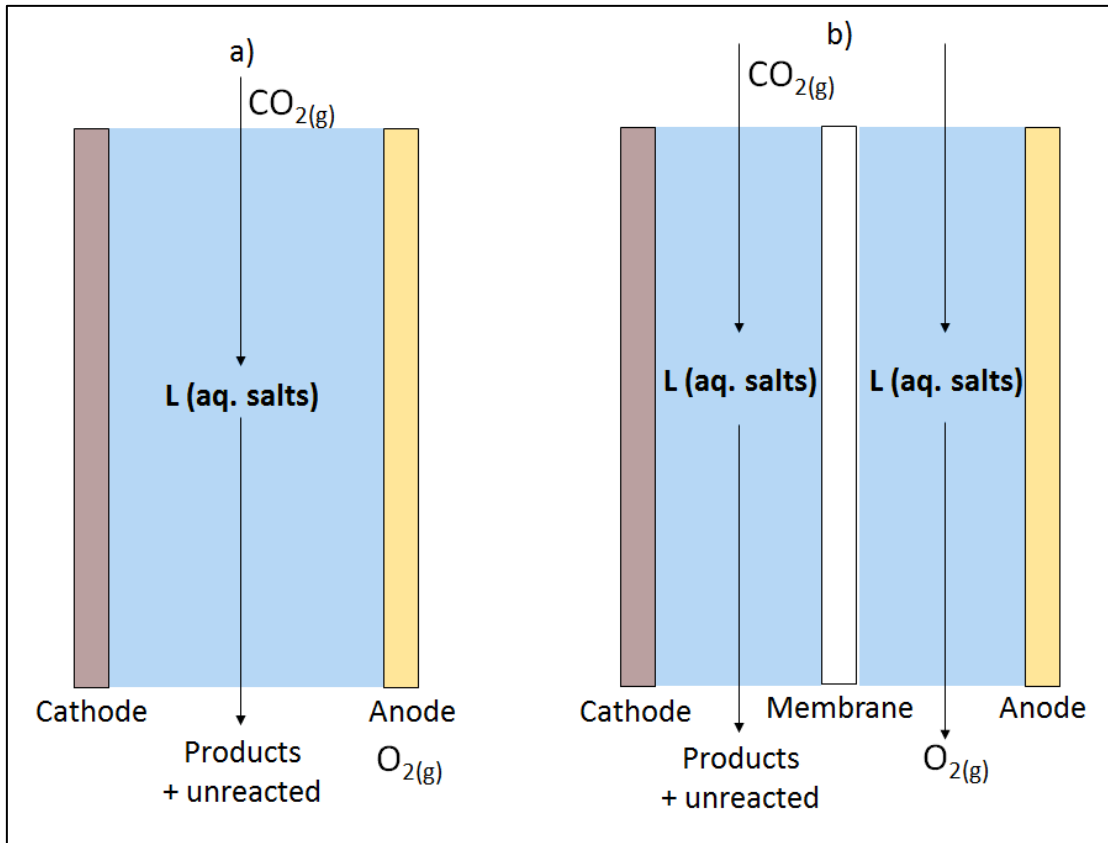
159

160 **3. Electrocatalytic membrane reactors**

161 The main limitations of CO₂ valorisation processes are related to the slow kinetics of
162 CO₂ electroreduction, high-energy consumption and low *EE* of the process. To tackle
163 those issues, different reactor configurations have been developed, in order to enhance
164 process performance and bring the technology for CO₂ electroreduction closer to the
165 industrial-scale [18].

166 This section analyses the different electrochemical reactor reported in literature, paying
167 special attention to the relative position of the electrodes and the membrane in each
168 configuration. The different reactor configurations applied along the time are presented
169 in Figures 4 to Figure 7.

170 Firstly, undivided electrochemical reactors, in which dense plates-type electrodes are
171 separated by a liquid phase that acts as both anolyte and catholyte (Figure 4.a) were
172 conventionally applied. In these cells, product recuperation is not simple and requires an
173 additional separation step, increasing process costs.



174
175 Figure 4. Conventional undivided electrochemical reactor (a) and electrochemical
176 reactor separated by an ion exchange membrane (b).

177 Besides, Figure 4.b. shows an ecMR with two compartments divided by an ion
178 exchange membrane. In this case, the membrane isolates cathodic and anodic reactions,
179 which may occur simultaneously in an electrochemical process, leading to an enhanced
180 separation of products and the avoidance of re-oxidation reactions [11]. Different
181 research groups have applied plate electrodes in two-compartment cells separated with
182 an ion exchange membrane [19, 23, 24, 26-36]. In general, the application of CEMs,
183 where the transport of protons is favoured, is preferred [20, 23, 24, 26, 28-36] with

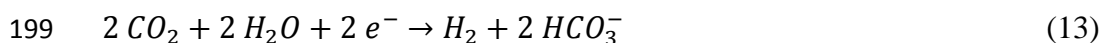
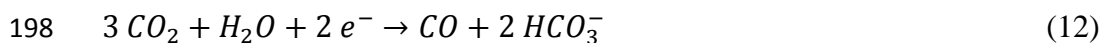
184 respect to the use of AEMs [19, 27], where species such as bicarbonate are mainly
185 transported through the membrane.

186 The type of membrane [11], together with the selection of the electrolyte (e.g. H^+ or K^+
187 can cross the membrane in H_2O or KOH aqueous anolytes, respectively), is very
188 important in the process. When a CEM is applied to the CO_2 electrochemical reduction
189 process, the following reactions are observed [11]:



192

193 However, with AEMs the anionic species travel from the cathode to the anode (e.g.
194 HCO_3^- from an aqueous solution of $KHCO_3$ as catholyte). In this case, CO_2 evolved at
195 the anode side and needs to be further separated from the O_2 generated in the anode.
196 The typical reactions for the CO_2 electroreduction to CO using AEMs at the cathode
197 side are as follows [11]:



200

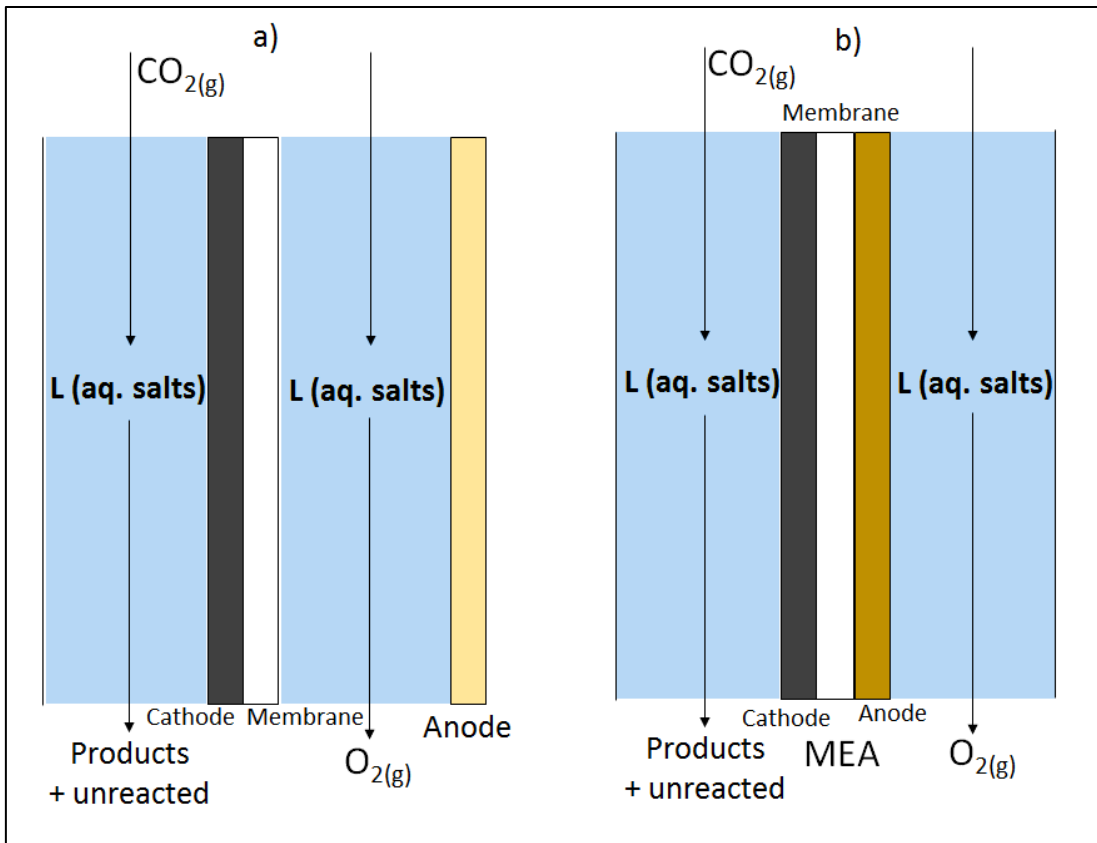
201 The main aspects that limit these electrochemical reactions are mass transport across the
202 membrane, the nature of the reaction medium and the required protons of the product of
203 interest. The procedure to activate the membranes prior their use is also a key factor to
204 achieve an enhanced CO_2 electrochemical reduction [37].

205 Besides, polarization losses in the electroreduction of CO_2 are usually related to the
206 transport of species and concentration gradients, which may basically depend on the
207 membrane. The effect of using a CEMs or AEMs on polarization losses was recently
208 studied by Singh et al. [38], concluding that losses when using a CEM are higher than

209 those for an AEM or without membrane. In spite of that, most of the works on CO₂
210 electrochemical reduction are performed with Nafion[®] CEMs. Other variables such as
211 cathode and anode overpotentials, mass transfer, pH between cathode and anode and
212 other operation conditions (e.g. CO₂ flow and pressure, *CD*, etc) should be also taken
213 into account in order to reduce polarization losses. In general, CO₂ reduction to CO
214 involves a high level of polarization. However, this level decreases as the number of
215 required electrons to produce a specific product increases. Besides, different ways to
216 minimize polarization losses, achieving high *CDs* to favour CO₂ reduction vs. hydrogen
217 evolution reaction (HER) have been proposed [38]. It seems that the electrolyte should
218 be close to neutral pH.

219 Moreover, in order to overcome mass transfer limitations occurring in ecMRs, GDEs, in
220 which the catalytic material is dispersed by different methods onto a porous structure,
221 have been used for the electrochemical valorisation of CO₂ [10, 21, 25, 39-44]. The
222 development of suitable supports to achieve a good catalyst dispersion and transport of
223 reactants (i.e. CO₂) is essential for an enhanced efficiency of the process. Porous carbon
224 papers have been usually applied for the fabrication of GDEs [39], although different
225 polymers, which enhanced properties, are currently under development [45].

226 Depending on the relative position of the GDE with respect to the ion exchange
227 membrane, different reactor configurations are reported (Figure 5). Particularly, Figure
228 5a shows a catalytic layer–membrane configuration [46]. Additionally, MEAs, where
229 cathode-membrane-anode are coupled and thus, the contact and transport of species
230 between the electrodes are enhanced, can be found in literature [11, 47-49].



231

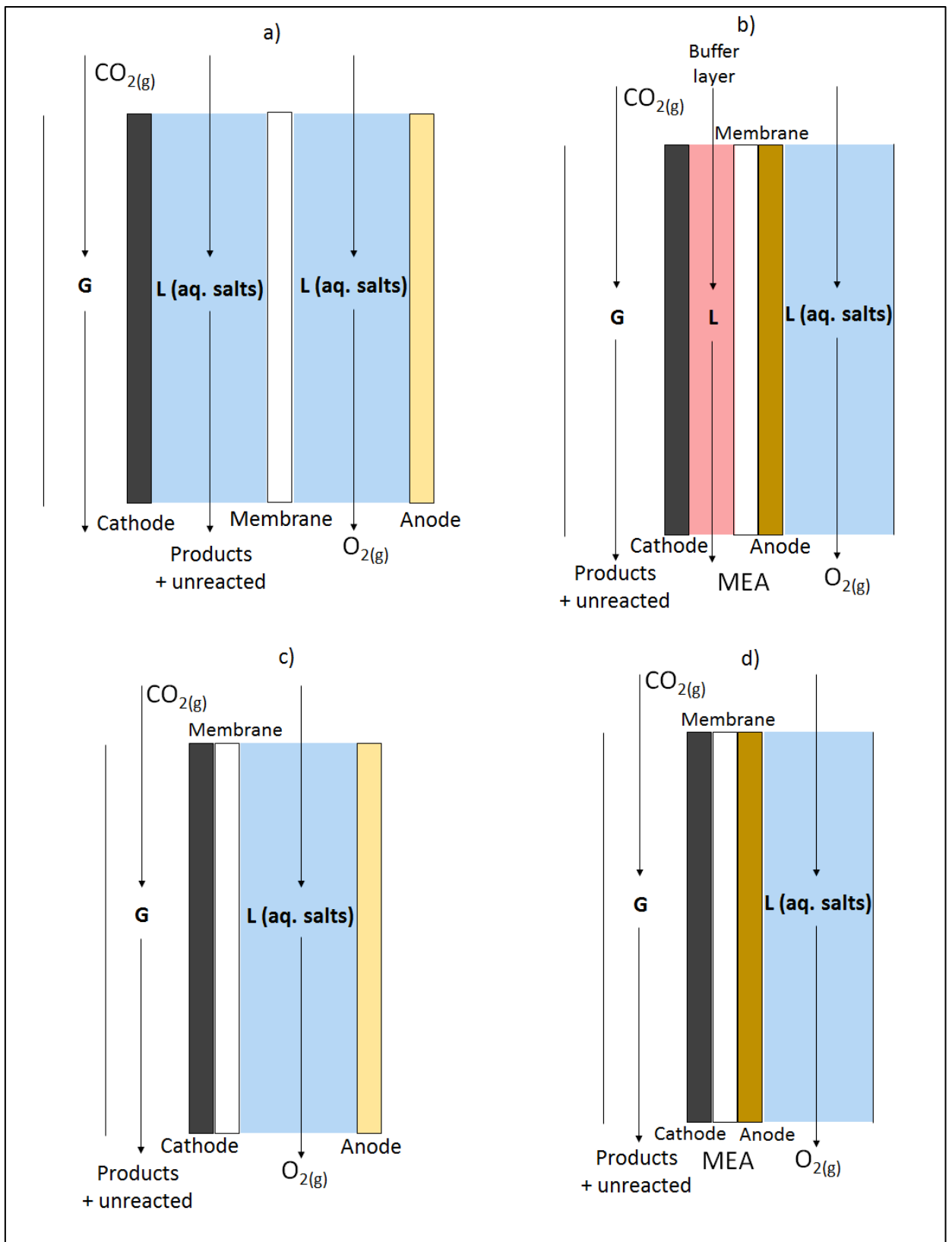
232 Figure 5. Catalysts dispersed at the cathode coupled with an ion exchange membrane (a)
 233 and, both electrodes coupled with the membrane (MEA) (b).

234 Furthermore, due to the low solubility of CO₂ in water and the possibility to avoid HER,
 235 the conversion of CO₂ directly in gas phase has aroused great interest recently [11, 22,
 236 50-57]. In this configuration, CO₂ transport resistances in the catholyte may be
 237 suppressed. Figure 6 shows different reactor configuration approaches using CO₂ gas at
 238 the cathode.

239

240

241



242
243

244 Figure 6. Different electrochemical reactor configurations for CO₂ valorisation in gas
245 phase: gas phase at the cathode separated to the catholyte (a), gas phase at the cathode

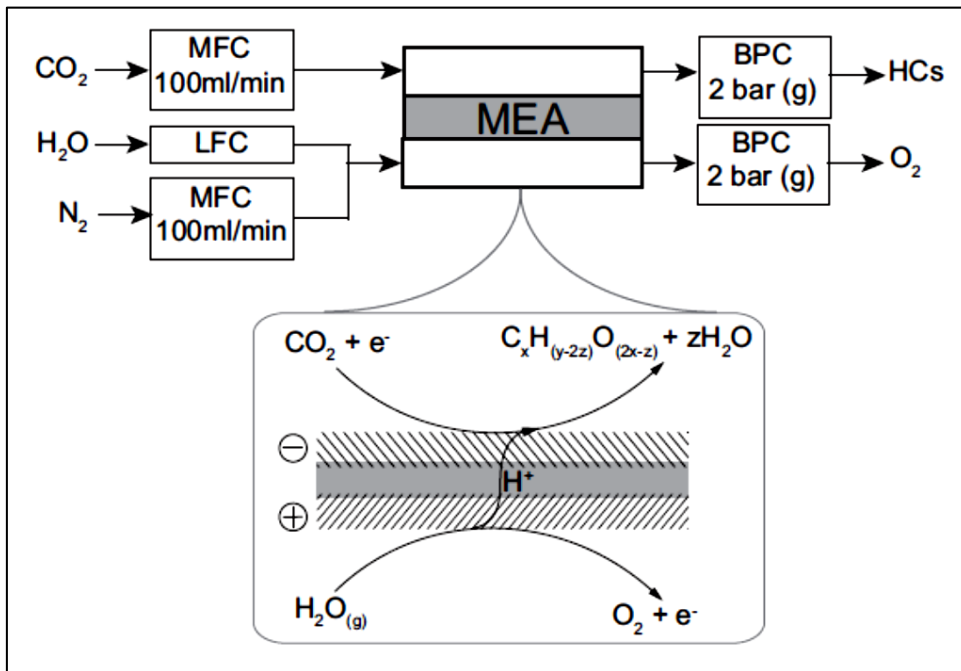
246 with a liquid buffer layer (b), cathode coupled to a membrane without buffer layer (c),
247 and MEA configuration (d).

248 The simplest configuration is shown in Figure 6.a, where a GDE is placed between the
249 gas stream and the catholyte, separating both phases. An alternative, is the replacement
250 of the catholyte by a pH-buffer layer (aqueous salt solution), usually applied between
251 the cathode and the membrane (Figure 6.b). This configuration permits the transport of
252 ionic species (i.e. H^+) by using different aqueous salts such as $KHCO_3$ [11, 50]. For
253 instance, a large increase in the selectivity for CO evolution (efficiency of 82 %) using
254 Ag-based catalyst as working electrode was observed with respect to a configuration in
255 which the buffer layer was not included [11]. Wu et al. [50] discussed that the inclusion
256 of a pH-buffer layer (0.1 M $KHCO_3$) allowed to dominate CO_2 reduction to $HCOO^-$ (*FE*
257 around 90 %) over HER using a sprayed Sn ink onto a GDL as cathode.

258 Figure 6.c and Figure 6.d present the cell configuration for the reduction of CO_2 in gas
259 phase. In the first case (Figure 6.c); the MEA contains a porous cathode coupled with
260 the membrane, with the anolyte solution between the anode and membrane [51-53]. In
261 the second configuration (Figure 6.d), the electrodes are sandwiched together with the
262 membrane (MEA) [11, 22, 54-57] facilitating the transport of ionic species, which may
263 be beneficial for an effective valorisation of CO_2 into more reduced products such as
264 CH_4 and C_2H_4 [17].

265 Finally, the development of electroreduction processes completely in gas phase at both
266 electrode compartments is under development. This configuration may overcome mass
267 transfer limitations and facilitate the separation of products. The available literature in
268 this regard is still scarce and it seems that further developments are required [13, 14].
269 Cook et al. [13] firstly developed gas-gas ecMRs for CO_2 reduction using a Nafion[®] 117
270 membrane. They observed the formation of CH_4 , C_2H_4 and C_2H_6 as major products.

271 Besides, Figure 7 shows the scheme of the electrocatalytic cell applied by Kriescher et
 272 al. [14] for CO₂ reduction to hydrocarbons.



273

274 Figure 7. Gas-gas ecMR used by Kriescher et al. [55]. Reproduced with permission
 275 from ref. [14].

276 The effect of temperature in the electroreduction of CO₂ to hydrocarbons was analysed
 277 when CO₂ and N₂ were supplied to the cathode and anode compartments, respectively.
 278 The applied MEA consisted on a Fumatech[®], Fumapem F-14001 CEM, a Cu-
 279 electrocatalyst (working electrode) and Ti covered with Ir as anode. The concentration
 280 of the desired product and current efficiencies were still very low (*FE* to CH₄= 0.12 %
 281 at 6 V and 70 °C). They finally suggest that a higher CO₂ residence time, the
 282 development of new membrane materials with high proton conductivity and low water
 283 transmission rates, and optimization of the three-phase interface (electrode, proton
 284 conductor and catalyst) may lead to an enhanced electroreduction of CO₂ in gas phase.
 285 In any case, further efforts in highly active catalysts, durability of the electrodes and
 286 new reactor configurations should be tackled in order to apply this technology for

287 technical applications. Finally, it is important to take into account the manufacture costs
288 associated to the fabrication of electrochemical reactors, which is not generally discuss
289 in the literature.

290

291 **4. Main results for CO₂ utilisation in ecMRs**

292 The section is divided in the two main electrochemical reactors: (i) Liquid-Liquid (L-L)
293 ecMRs (even though gas phase may be also present in the cathode side) and (ii) Gas-
294 Liquid (G-L) ecMRs (where gas phase is only in the cathode). Then the subsections are
295 divided by the nature of the membranes and the applied catalysts, in order to give an
296 overview of reported studies in terms of *FE*, *CD* and the voltage (*E*) required in each
297 process with similar catalyst-based materials and membranes.

298 *4.1. Liquid-Liquid (L-L) ecMRs*

299 Table 1 summarizes the type of membranes applied, catalytic materials and
300 experimental conditions in L-L ecMRs for the electrochemical reduction of CO₂. Most
301 of the reported studies employed proton conductive membranes (mainly Nafion[®]) to
302 separate catholyte and the anolyte, which usually consist of aqueous solutions of
303 KHCO₃ and KOH, respectively [10, 11, 20, 21 23, 24, 26, 28-35, 40-43, 46, 47, 49, 58-
304 67] in comparison to those reports where cathode and anode chambers are separated by
305 an AEM [19, 27, 36, 54, 68, 69].

306 As it can be seen, CO, HCOOH, CH₄ and C₂H₄ are the most common products in L-L
307 ecMRs. Besides Ag, Sn or Pb, and Cu-based electrodes are the common catalysts
308 applied, since they allow to obtain CO, HCOOH and hydrocarbons, respectively, with
309 high *FEs*.

310 The following subsections critically discuss the reported L-L ecMRs reactors according
311 to the type of membranes and catalysts applied in the CO₂ electroreduction process.

312 Table 1. Experimental conditions, catalytic materials, main products and significant results for CO₂ valorisation in L-L ecMRs.

Membrane	Cathode	Anode	Catholyte	Anolyte	Products	V vs. Ag/AgCl / CD (mAcm ⁻²)	Main results	P (atm) / T (°C)	Ref.
Nafion®	Sn-GDE	Pt plate	CO ₂ , KHCO ₃	aq. KHCO ₃	HCOOH, H ₂ , CO, CH ₄	50 mA/cm ²	FE HCOOH= 93 %	1 / 25	[10]
Nafion®	Ag	Pt-Ir (1:1) alloy	CO ₂ , KHCO ₃	aq. KOH	CO, H ₂	-1.38 V	FE CO= 40 %	1 / 25	[11]
Selemion™ (AEM)	Ag foil	Pt foil	CO ₂ , KHCO ₃	aq. KHCO ₃	CO, H ₂ , HCOOH, CH ₄ , CH ₃ OH, C ₂ H ₅ OH	-1.6 to -1.3 V	FE CO= 90 %; HCOOH= 8 %	1 / 25	[19]
Nafion® 117	Pb plate	DSA	CO ₂ , KCl + KHCO ₃	aq. KOH	HCOOH	2.5 mAcm ⁻²	FE HCOOH= 94.7 % (14.4 mg/L)	1 / 25	[20]
Nafion® 117	Cu ₂ O	Platinized titanium	CO ₂ , KHCO ₃	aq. KHCO ₃	CH ₃ OH	-1.3 V	FE CH ₃ OH= 45.7 %	1 / 25	[21]
Nafion® 450	Mesh tinned-Cu plate	Platinized titanium plate	CO ₂ y N ₂ , KHCO ₃	aq. KOH	HCOOH, H ₂ , CO, CH ₄	22 mAcm ⁻²	FE HCOOH= 86%	1 / 25	[23]
Nafion® 117	Sn plate	DSA	CO ₂ , KCl + KHCO ₃	aq. KOH	HCOOH	12.25 mAcm ⁻²	FE HCOOH= 70 %	1 / 25	[24]
Polymer electrolyte membrane	Pt-Glassy carbon electrode	Pt wire	Deionized water or KHCO ₃	Pure deionized water	HCOOH	-	HCOOH: continuous mode (0-35 mM); discontinuous mode (0-18 mM)	1 / 25	[25]
Nafion® 117	Cu foil	Pt foil	CO ₂ , LiOH in CH ₃ OH	KOH in CH ₃ OH	CH ₄ , C ₂ H ₄ , CO, HCOOH	-4 V	FE (CH ₄ + C ₂ H ₄)= 78 %	- / -30	[26]
Selemion™ (AEM)	Cu foil	Pt foil	CO ₂ , KHCO ₃	aq. KHCO ₃	16 different products	-1.35 to -1.07 V	FE CH ₄ = 40 %; C ₂ H ₄ = 25 %; HCOOH= 23 %	-	[27]
Nafion® 112	Cu ₂ O films	Pt mesh	CO ₂ , KHCO ₃	aq. KHCO ₃	C ₂ H ₆ , C ₂ H ₄ , CH ₄ , CO	-1.3 V	FE C ₂ H ₄ = 20 %; CH ₄ = 5 %; CO= 4 %; C ₂ H ₆ = 2.5 %	1 / 25	[28]
Nafion® 117 or no membrane	Cu plate	Pt plate	CO ₂ , NaOH or KOH in CH ₃ OH	NaOH or KOH in CH ₃ OH	CH ₄ , H ₂	-	Without membrane and using KOH: FE CH ₄ = 35.6 %	1.2 / 25	[29]
Nafion® 117	Pt/Nb plate	Pt/Nb	CO ₂ , CH ₃ OH	CH ₃ OH +	DMC	-	DMC: 11.37 mM	-	[30]

	(95% Pt)	plate (95% Pt)	+ [bmim][Br] + CH ₃ OK	[bmim][Br] + CH ₃ OK					
CEM	Modified Cu electrodes	Pt mesh	CO ₂ , KHCO ₃	aq. KHCO ₃	CH ₄ , C ₂ H ₄ , C ₂ H ₆ , H ₂ , CO	-1.9 V	FE C ₂ H ₄ = 33 %; CH ₄ = 10 %	1 / 25	[31]
CEM	Cu mesh	Pt mesh	CO ₂ , KHCO ₃	aq. KHCO ₃	CH ₄ , C ₂ H ₄ , C ₂ H ₆ , H ₂ , CO	-1.9 V	FE CH ₄ = 15 %; C ₂ H ₄ = 8 %	1 / 25	[32]
Nafion® 117	Cu foil	Pt foil	CO ₂ , sodium salts in CH ₃ OH	KOH in CH ₃ OH	CH ₄ , C ₂ H ₄ , HCOOH, CO, H ₂	-3 V	FE CH ₄ = 70.5 % in NaClO ₄ /CH ₃ OH	- / -30	[33]
Nafion® 117	Cu wire	Pt plate	CO ₂ , LiClO ₄ in CH ₃ OH	aq. H ₂ SO ₄	CH ₄ , C ₂ H ₄ , CO, HCOOH, CH ₃ COOH	*-3 V	20 bar: FE CH ₄ = 25.5 %; CO= 15.1 %; HCOOH= 22.1 %; CH ₃ COOH= 40.2 %	1-60 / -	[34]
Selemion™ (CEM)	Cu-halide electrodes	Pt plate	CO ₂ , potassium halides	aq. potassium halides	CH ₄ , C ₂ H ₄ , C ₂ H ₆ , CO, C ₂ H ₅ OH, H ₂	-2.4 V	CuBr electrode and KBr electrolyte: FE C ₂ H ₄ = 79.5 %; CH ₄ = 5.8 %	-	[35]
FAB (AEM) or no membrane	Pt/Nb plate (95% Pt)	Pt/Nb plate (95% Pt)	CO ₂ , CH ₃ OH + [bmim][Br] + CH ₃ OK	CH ₃ OH + [bmim][Br] + CH ₃ OK	DMC	-	Undivided cell: 80.85 mM; FAB membrane: 9.74 mM	-	[36]
Nafion® 117	Sn-GDE	DSA	CO ₂ , KCl + KHCO ₃	aq. KOH	HCOOH	---	FE HCOOH= 70 % (1348 mg/L)	1 / 25	[40]
Nafion® 117	Sn-GDE	Pt foil	CO ₂ , KHCO ₃	Water	HCOOH	-1.8 V	FE HCOOH= 78 %	- / 25	[41]
Selemion™ (CEM)	Net Ag-electrode	Pt plate	CO ₂ , KCl	aq. KCl	CO, H ₂	-	AgNO ₃ added to the electrolyte). FE CO> 45 %	-	[42]
Nafion®	Sn-GDE + PTFE	Pt foil	CO ₂ , KHCO ₃	aq. KHCO ₃	HCOOH	-1.8 V	FE HCOOH= 87 %	- / 25	[43]
Nafion® 117	Pt NP-CNT	Pt rod	CO ₂ , KHCO ₃	aq. KHCO ₃	HCOOH, CH ₃ COOH	-	HCOOH= 2.3x10 ⁻⁴ M; CH ₃ COOH= 1.8x10 ⁻⁴ M	- / 25	[46]
Nafion® 117	Ag - Graphite GDL	Pt black NP	CO ₂ , [emim][Br]	aq. H ₂ SO ₄	CO, H ₂	-1.5 V	FE CO> 9 % (H ₂ balance)	- / 22	[47]
Nafion® 117	Ag NP	Pt NP	CO ₂ , Aq. [bmim][BF ₄]	aq. H ₂ SO ₄	CO	-	FE CO~ 100 % when 89.5 mole% water was added to the [bmim][BF ₄]	-	[49]
Selemion™ (AEM)	Cu mesocrystals	Pt mesh	CO ₂ , KHCO ₃	aq. KHCO ₃	HCOOH, CH ₄ , C ₂ H ₄ , CO, H ₂	-1.4 to -0.9 V	FE C ₂ H ₄ = 27.2 %; HCOOH= 17.5 %; CO= 7.5 %; CH ₄ = 2.7 %	-	[54]
Nafion® 961 and Nafion® 430	Pb plate	IrO ₂ /Ta ₂ O ₅	CO ₂ , K ₂ HPO ₄ + H ₃ PO ₄	Aq. KOH	HCOOH	2 mAcm ⁻²	FE HCOOH= 93 % HCOOH at 2 mA/cm ² . HCOOH concentration increases with CD (max.= 0.016 M)	1 / 25	[58]

Nafion®	Electrocatalysts: Cu, CuO, ZnO, Mo ₂ C, Co ₃ O ₄	Pt/C (40% wt)	CO ₂ , KHCO ₃ or KOH or DMF	Water	-	-	Cu, CuO, ZnO, Co ₃ O ₄ actives catalysts in the protocol	1 / 25	[59]
Nafion® 112	Cu NWs or Cu NNs	Pt foil	CO ₂ , KHCO ₃	aq. KHCO ₃	CH ₄ , C ₂ H ₄ , HCOOH, H ₂	-1.5 to -1.1 V	Cu NWs: FE C ₂ H ₄ = 12%; Cu NNs: FE CH ₄ = 14 % and HCOOH= 48 %	- / 10	[60]
Selemion™ (CEM)	Cu	-	CO ₂ , KHCO ₃	aq. KHCO ₃	CH ₄ , C ₂ H ₄ , CO, HCOOH	-1.64 V	FE CH ₄ = 33.3 %; C ₂ H ₄ = 25.5 % at - 1.44V and 5 mA/cm ²	- / 19	[61]
CEM	Crystal Cu	-	CO ₂ , KHCO ₃	aq. KHCO ₃	CH ₄ , C ₂ H ₄ , CO, HCOOH, H ₂ , alcohols	-1.75 V	Cu (110): FE CH ₄ = 49.5 %; C ₂ H ₄ = 15.1 %	- / 18	[62]
Nafion® 117	Sn-GDE	DSA	CO ₂ , KCl + KHCO ₃	aq. KOH	HCOOH	-2 V / 90 mAcm ⁻²	FE HCOOH=70 % (1519 mg/L)	1 / 25	[63]
Selemion™	Cu NP over glassy carbon	-	CO ₂ , NaHCO ₃	aq. NaHCO ₃	CH ₄ , H ₂	-1.55 V	FE CH ₄ = 76 %	1.2 / 25	[64]
Nafion® 112	Cu ₂ O electrodeposited	Pt mesh	CO ₂ , KHCO ₃	aq. KHCO ₃	CH ₄ , C ₂ H ₄ , H ₂ , CO, HCOOH	-1.9 V	FE CH ₄ = 21 %; C ₂ H ₄ = 11 %; H ₂ = 50 %	1 / -	[65]
Nafion®	Cu foil	Pt mesh	CO ₂ , KHCO ₃	aq. KHCO ₃	CH ₄ , C ₂ H ₄ , H ₂ , CO	-1.65 to -1.4 V	FE CH ₄ = 0-70 %; C ₂ H ₄ = 0-35 %; H ₂ = 10-95 %; CO= 0-13%	-	[66]
Nafion®	Fe NP over GDL	Pt wire	CO ₂ , KHCO ₃	aq. KHCO ₃	HCOOH, CH ₃ COOH, CH ₃ OH	**1 V	Global productivity: 1.75x10 ⁻² mmole/h	- / 25	[67]
Selemion™ (AEM)	Cu ₂ O-derived Cu	Pt wire	CO ₂ , KHCO ₃ , PdCl ₂	aq. KHCO ₃	C ₂ H ₆ , H ₂ , alcohols, CH ₄ , C ₂ H ₄ , CO	-1.2 V	FE C ₂ H ₆ = 30 %; H ₂ = 15 %; alcohols< 15 %; CH ₄ , C ₂ H ₄ and CO= traces	-	[68]
Selemion™ (AEM)	Cu ₂ O layers into Cu disc	Pt wire	CO ₂ , KHCO ₃	aq. KHCO ₃	C ₂ H ₄ , H ₂ , C ₂ H ₅ OH, CH ₄ , CO, HCOOH	-1.2 V	FE C ₂ H ₄ = 39 %; H ₂ ~ 50 %; rest of products< 10 %	-	[69]

313
314

* Ref. electrode: Pb(Hg)x/PbSO₄/SO₄²⁻

** Difference of 1 V between electrodes

315 4.1.1. L-L ecMRs based on CEMs

316 CEMs have been widely used in ecMR systems due to their enhanced properties for the
317 transport of protons. Among the available materials, Nafion[®] is typically applied. A
318 number of value-added products, on dependence of the electrocatalytic materials
319 applied, can be found in the literature as described hereafter.

320 Ag-based electrodes

321 In the first group, silver cathodes have been commonly used for CEM-based systems
322 [11, 42, 47-49]. In this regard, Delacourt et al. [11] studied different reactor
323 configurations for the electrochemical reduction of CO₂ to syngas (CO + H₂). A
324 Nafion[®] membrane was used in a L-L ecMR to form a MEA. The catalytic layer
325 consisted in acetylene black carbon and a polymer of the same nature, together with Ag
326 catalyst. The experiments were carried out at 20 mA·cm⁻² with a cathode potential of -
327 1.42 V vs. SCE. A CO formation efficiency of 40% was achieved. In the same way,
328 other researchers have also used different CEMs for the electrochemical reduction of
329 CO₂ to syngas [42, 47-49].

330 Rosen et al. [47] applied a sandwich style reactor with two liquid and gas channels with
331 a Nafion[®] 117 membrane. An Ag nanopowder ink supported on Sigracet graphite GDL
332 was used. The ionic liquid [emim][Br] was used as catholyte, obtaining a *FE* to CO
333 higher than 96 % as a function of the potential cell applied. Besides, *FE* to H₂ formation
334 was very low. The *EE* observed ranged between 50 % to 90 % at 1.5 V. Salehi-Khojin
335 et al. [48] also used a Nafion[®] membrane in a L-L ecMR. The rate for CO₂ conversion
336 was about 10 times higher on 5 nm Ag nanoparticles (NP) than on a bulk Ag electrode.

337 Moreover, Rosen et al. [49] also used Ag NP and the ionic liquid [emim][BF₄] for the
338 electroreduction of CO₂. They showed that the addition of water to the ionic liquid

339 increased the efficiency for CO₂ conversion to CO. The maximum *FE* to CO achieved
340 in this system was nearly 100 % when 89.5 mol% water was added to the ionic liquid.
341 Besides, Yano et al. [42] used a SelemionTM CEM to separate the cathode and anode
342 compartments, with a GLS (gas-liquid-solid)/Ag electrode and 0.5 M KCl. The effect of
343 the pH was studied. The *FE* to CO was higher than 45 % using a GLS-Ag electrode.
344 Besides, a CO conversion near 100 % was observed when AgNO₃ was added to the
345 electrolyte at pH=3.5, concluding that *FE* decreased as the pH increased.

346 Overall, it seems that an appropriate catholyte and pH conditions are crucial for an
347 enhanced CO₂ electrochemical conversion. Besides, the application of highly
348 conductive ionic liquids for the reduction process seems to be beneficial [70]. The use
349 of CEMs for the electrochemical reduction of CO₂ to CO in Ag-based electrodes in
350 combination with ionic liquids as electrolytes showed *FEs* to CO near to 100 %.

351 Cu-based electrodes

352 Moreover, several authors reported the application of Cu-based catalysts in combination
353 with CEMs for the electrochemical reduction of CO₂ into valuable products [21, 23, 26,
354 28, 29, 31-35, 46, 59-62, 64-66, 71]. The conversion efficiencies have been found to be
355 directly linked to the type of Cu catalyst used in the working electrode (Cu foil, Cu
356 mesh, Cu NP, etc).

357 Ogura et al. [71] describe a Cu mesh in order to evaluate the influence of different
358 potassium halides (KCl, KBr and KI) as catholytes at pH=3. A Nafion[®] 117 membrane
359 was used to divide the anode and cathode compartments. They concluded that the
360 presence of Cu-halide anions facilitated the electron transfer and the current density.
361 The reduction of CO₂ increases in the following order Cl⁻ < Br⁻ < I⁻. A tinned-Cu mesh
362 cathode together with a Nafion[®] 450 membrane has also been proposed to electroreduce

363 CO₂ to HCOOH, H₂, CO and CH₄ in L-L ecMR [23] with a pure CO₂, or a mixture of
364 CO₂ and N₂, in gas phase combined with a 0.45 M KHCO₃ catholyte. The experiments
365 were carried out near ambient conditions and over a *CD* range of 22 to 178 mA·cm⁻².
366 The *FE* achieved for each product in the factorial design of experiments carried were
367 23-71 % to HCOOH, 24-86 % to H₂, 0-5 % to CO and 0-0.3 % to CH₄. They also
368 showed that current efficiency increases with CO₂ concentration. The maximum *FE* to
369 HCOOH (*FE*= 86%) was obtained at 22 mA·cm⁻². Kas et al. [28] used a three-electrode
370 assembly in order to analyse the catalytic activity for the electrochemical reduction of
371 CO₂ to hydrocarbons. Cuprous oxide films were electrodeposited onto Cu plates as
372 working electrodes, with a Nafion[®] 112 membrane separating the cathode and anode
373 compartments. A 0.1 M KHCO₃ solution (pH= 6.8) was used as catholyte with CO₂ gas
374 to produce CO, CH₄, C₂H₄ and C₂H₆ at a *FE* of 0-4%, 1-5%, 20% and 2.5%,
375 respectively, at an applied voltage of -1.1 V vs. RHE.

376 Gonçalves et al. [31, 32] evaluated a Cu mesh and a modified Cu electrode for the
377 reduction of CO₂. The Cu-modified materials showed an improved efficiency for the
378 electrochemical reduction of CO₂ to hydrocarbons, in comparison to a Cu mesh, with a
379 *FE* as high as 33% and 10% for C₂H₄ and CH₄, respectively. Manthiram et al. [64]
380 demonstrated that well-dispersed Cu NP over glassy carbon (working electrode) show
381 high *FEs* to CH₄ from CO₂ reduction using a two-compartment flow cell. A Selemion[™]
382 membrane separated the working and counter electrode compartments, which are filled
383 with an aqueous solution of 0.1M NaHCO₃. A *FE* to CH₄= 76 % was obtained at -1.55
384 V vs. Ag/AgCl, higher than the obtained values at Cu foils for the same conditions (*FE*~
385 40 %). The authors suggested that these prepared Cu-electrodes may help to achieve
386 enhancement for the electrochemical reduction of CO₂ to CH₄, minimizing polarization
387 losses and maximizing the energy efficiency.

388 Moreover, Kas et al. [65] suggested that the concentration of the electrolyte could
389 strongly affects the selectivity of the electrochemical reduction of CO₂ to hydrocarbons.
390 Cu-NP over Cu substrates were used as working electrodes in a two-compartment
391 stainless-steel autoclave reactor, in which a Nafion[®] 112 membrane divided the cathode
392 and anode (Pt mesh) compartments. A 0.5 M KHCO₃ aqueous solution allows to obtain
393 *FES* of 21 %, 11 % and 50 % to CH₄, C₂H₄ and H₂, respectively, at -1.9 V vs. Ag/AgCl
394 and 1 atm. However, decreasing the electrolyte concentration to 0.1 M results in
395 increased *FE* to C₂H₄ (36 %) in the same conditions. Besides, C₂H₄ formation is
396 additionally favoured by increasing CO₂ pressure to 9 atm. From these results, it can be
397 concluded that the concentration of the electrolyte has an important effect in the
398 selectivity of the electrochemical reduction of CO₂ into hydrocarbons. The same idea
399 was supported by Varela et al. [66] in an H-type cell divided by a Nafion[®] membrane
400 using the same electrolyte (aq. KHCO₃ solution). A Cu foil and a Pt mesh were used as
401 working and counter electrodes, respectively. The maximum *FE* to CH₄ (70 %) was
402 obtained at -1.6 V vs. Ag/AgCl, applying a 0.2 M KHCO₃ concentration as electrolyte.
403 According to the work developed by Kas et al. [65], electrolytes with high buffer
404 capacity (i.e. high KHCO₃ concentration) increase *FE* to CH₄ and H₂ over C₂H₄. They
405 also add that C₂H₄ formation is not affected by local pH at low overpotentials
406 (proton/electron transfer is not the rate determining step in the formation process).

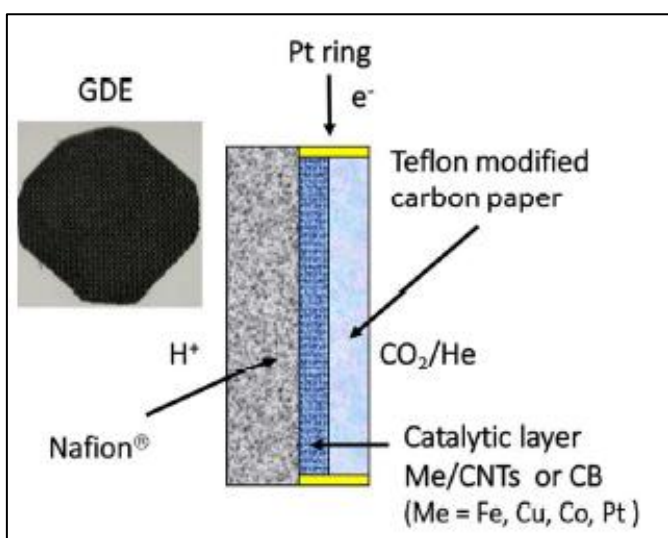
407 Kaneco et al. used a Cu foil as cathode with different sodium salts in CH₃OH [33] or
408 LiOH [26]. A Nafion[®] 117 membrane was used in both cases to separate the cathode
409 and anode sides, and high negative V vs. Ag/AgCl were applied to the cell. When a
410 NaClO₄ /CH₃OH mixture was used as electrolyte [33] the *FE* to CH₄ was 70.5 % at -3
411 V. In the second case [26], the *FE* to CH₄ + C₂H₄ was as high as 78 % at -4 V. The
412 positive effect of sodium salts in CH₄ selective production was then proven. Aydin et al.

413 [34] used a Cu wire with polypyrrol-coated electrocatalyst. A lithium salt (LiClO_4) in
414 methanol was used as catholyte with a Nafion[®] 117 membrane separating the chambers.
415 High-pressure experiments (10, 20, 40, and 60 bars) in a CO_2 atmosphere were
416 performed. At 20 bar, *FE* was as high as 25.5 % and 3.1 % for CH_4 and C_2H_4 ,
417 respectively. Other different products such as CO , HCOOH and acetic acid were also
418 detected with a *FE* of 15.1 %, 22.1 % and 40.2 %, respectively. Yano et al. [35] used a
419 CEM (Selemion[™]) and a Cu mesh or Cu (I) halide-confined mesh with the same
420 catholyte and anolyte based on aqueous potassium halides. The study seeks to analyse
421 the influence of different Cu-halides electrodes at -2.4 V vs. Ag/AgCl applied potential.
422 The CuBr electrode presented higher *FE* to C_2H_4 when KBr was used as electrolyte
423 (*FE*= 79.5 % and 5.8 % to C_2H_4 and to CH_4 , respectively). CuI and CuCl have been also
424 used as electrodes in this system, and the *FE* to C_2H_4 in each case was 72.8 % and 60.5
425 %, respectively. The study showed that Cu halide-confined meshes enhance the *FE* to
426 C_2H_4 in comparison to a Cu mesh electrode (*FE* of 40% to C_2H_4 in KCl solution).

427 Xie et al. [60] used a two compartment cell based on modified Cu electrodes (Cu
428 nanowires or Cu nanoneedles), 0.1 M KHCO_3 as electrolyte and a Nafion[®] 112
429 membrane to separate the compartments. Cu nanowires presented better results in terms
430 of *FE* to C_2H_4 (12% at -1.3 V vs. RHE) whereas Cu nanoneedles led to the highest *FE*
431 to CH_4 (14 % at -1.2 V) and to HCOOH (48 % at -0.9 V). Hori et al. [61, 62] also used a
432 CEM to separate the cathode and the anode in L-L ecMRs. The performance of different
433 metal electrodes as cathode catalyst [61] and different Cu single crystal electrodes [62]
434 were studied to analyse their influence in CH_4 and C_2H_4 production. The highest *FE*
435 was observed for a Cu electrode at -1.44 V vs. NHE at $5 \text{ mA}\cdot\text{cm}^{-2}$ (33.3 % CH_4 and
436 25.5 % C_2H_4) [61]. In a second study [62], higher *FEs* to CH_4 were achieved when a Cu
437 (110) electrode was used (49.5% CH_4 and 15.1% C_2H_4 at -1.55 V and $5 \text{ mA}\cdot\text{cm}^{-2}$). The

438 influence of *CD* in the *FE* to hydrocarbons was also tested. At low current densities (2.5
 439 mA·cm⁻²), the *FE* to hydrocarbons dropped, so high *CDs* were needed in these systems.
 440 Higher *FE* to CH₄ and to C₂H₆ were observed in an H-type electrochemical cell divided
 441 by a glass frit [72] using pure or electrodeposited Cu, which were carried out in CuSO₄
 442 0.25M (Cu/Cu-H) or 0.025 M (Cu/Cu-L) baths. Results with a pure Cu electrode
 443 showed that *FE* to CH₄ was about 28 % at -1.2 V and *FE* to C₂H₆ was about 15 % at -1
 444 V. The highest *FE* to C₂H₆ in this work was achieved on Cu/Cu-L electrodes with a
 445 value about 43 % at -1.2 V. When a Cu/Cu-H electrode was used, a *FE* to CH₄ and to
 446 C₂H₆ about 20 % and 27 %, respectively, was observed at -1.2 V [72].

447 Ampelli et al. [46] studied the influence of the phase used in the cathode in order to
 448 carry out a comparison in terms of productivity and type of products at the same
 449 conditions (electrodes and reaction). In these reactors, a Nafion[®] membrane was used to
 450 separate the compartments and different metal NP such as Co, Cu, Fe and Pt were
 451 supported over functionalized carbon nanotubes (CNTs) or commercial carbon black
 452 (CB), forming a GDE as represented in Figure 8. The differences between the systems
 453 are the type of electrolyte at the anode compartment (KHCO₃ in L-L ecMR and KCl in
 454 G-L ecMR).



455

456 Figure 8. Representation of the GDE used for CO₂ electrochemical reduction in the
457 work from Ampelli et al. [46]. Reproduced with permission from ref. [46].

458 Different products were detected in each configuration. HCOOH, acetic acid and
459 CH₃OH were obtained as traces in the L-L ecMR. In addition, the order of product
460 formation was on dependence of the metal catalyst applied: Pt-CNT ~ Fe-CNT > Cu-
461 CNT > Fe-carbon black in the L-L ecMR. In addition, the reaction mechanisms were
462 analysed in both cases [46]. The absence of the electrolyte and the higher CO₂
463 concentration at the catalyst surface could inhibit the mechanisms for electron transfer,
464 favouring the CO₂ dissociation to CO at the different metals used as catalyst.

465 Yim et al. [29] studied the influence of the membrane in a L-L ecMR using CH₃OH as a
466 solvent. A Cu plate was used as cathode, and a Nafion[®] 117 membrane for CH₄
467 production. The results showed that the electrochemical cell without membrane
468 presented better results (*FE*= 35.6% to CH₄) in comparison to the system with the
469 Nafion[®] membrane.

470 Albo et al. [21] studied the electrochemical reduction of CO₂ into CH₃OH using Cu₂O
471 and Cu₂O/ZnO-catalyzed carbon papers. A Nafion[®] 117 membrane was also used to
472 separate the cathode and anode compartments. When a Cu₂O-carbon paper electrode
473 was used, a *FE* to CH₃OH of 45.7 % was achieved, but a rapid deactivation of the
474 material occurred. In any case, a stable modest *FE* of 17.7 % was obtained in Cu₂O/ZnO
475 (1:1)-based systems at -1.3 V vs. Ag/AgCl, so the use of Cu₂O-ZnO mixtures for the
476 continuous electrochemical CO₂ reduction to CH₃OH showed promise. Recently, the
477 technical possibilities for the electrochemical reduction of CO₂ into CH₃OH has been
478 reviewed [73].

479 Regarding the possibility of suppressing the liquid phase from the catholyte (to avoid
480 transfer limitation due to the low solubility of CO₂ in water), Genovese et al. [67] made
481 a comparison between liquid (L-L ecMR) and gas (G-L ecMR) conditions in the
482 production of fuels from CO₂ reduction. Different metallic NP (Fe or Cu) supported on
483 GDL were tested as working electrodes, whereas a Pt wire was used at the anode side. A
484 CEM (Nafion[®]) divided the cell compartments filled with a 0.5 M KHCO₃ solution in
485 the anode side. Alcohols and traces of hydrocarbons were observed in gas-phase
486 studies, while liquid phase experiments mainly produced HCOOH, CH₃COOH and
487 traces of CH₃OH. As a conclusion, liquid phase CO₂ reduction allowed to achieve
488 higher productivity values (5×10^{-3} mmol·h⁻¹ in liquid phase over 1.5×10^{-4} mmol·h⁻¹ in
489 gas phase, using Cu-GDL-based catalyst), minimizing also the HER.

490 As can be deduced from the discussion above, the catalyst plays a main role in the
491 electrochemical reduction of CO₂, so a correct catalyst selection for each process is
492 essential. For this purpose, Singh et al. [59] developed a catalytic activity protocol for
493 the electrochemical reduction of CO₂. Different electrocatalysts (Cu, CuO, ZnO, Mo₂C
494 and Co₃O₄) were supported into a GDL, forming the cathodes. A Nafion[®] membrane
495 was sandwiched between the electrodes and different studies such as cyclic
496 voltammetry (CV) and linear sweep voltammetry (LSV) were carried out, whilst the
497 cathode side of the reactor was fed with CO₂ saturated 0.5 M KHCO₃ solution. As
498 conclusion, Cu, CuO, ZnO and Co₃O₄ were actives in the proposed protocol for the
499 electrochemical reduction of CO₂.

500 In conclusion, Cu-based electrodes have been widely used as cathodes. It seems that
501 nanomaterial-based electrodes may enhance the electroreduction of CO₂ to
502 hydrocarbons (mainly CH₄ and C₂H₄) [64]. Besides, electrolyte type and its
503 concentration seem to be crucial for an efficient CO₂ electroreduction process. Finally,

504 the utilisation of Cu-halides meshes is favourable, attending to the high *FE* to C₂H₄
505 (79.5 %) in L-L ecMRs divided by a CEM, in comparison to the *FE* achieved on Cu-
506 mesh electrodes [35].

507

508 *Sn and Pb-based electrodes*

509 Many authors have focused their research on the utilisation of tin and lead catalysts for
510 the electroreduction of CO₂ using L-L ecMRs [10, 20, 24, 40, 41, 43, 58, 63] with the
511 aim of producing HCOOH with high *FEs*. Kopljar et al. [10] studied the feasibility of
512 the electrochemical HCOOH production within an industrial environment. A proton
513 conductive membrane (Nafion[®]) to separate the cathode and anode chamber was used
514 and both chambers were filled with an aqueous solution of KHCO₃. High *FE* (> 80 %) was
515 obtained at 200 mA·cm⁻² and pH= 10, whereas the *FE* for CO and H₂ was
516 approximately 10 %. A maximum *FE* of 93 % to HCOOH was achieved at 50 mA·cm⁻².
517 In the same way, Wang et al. [41] carried out different electrochemical measurements
518 such as CV and electrochemical and impedance spectroscopy (EIS), in order to analyse
519 the *FE* to HCOOH formation. The electrolyte was a KHCO₃-based solution in a wide
520 range of concentrations. When a concentration of KHCO₃ equal to 0.5 M is used, a
521 maximum *FE* of 78 % to HCOOH was achieved at an applied potential of -1.8 V. Wang
522 et al. [43] reached performance enhancements by adding polytetrafluoroethylene
523 (PTFE) into the catalyst layer. This makes possible to increase the catalytic surface area
524 and CO₂ diffusion. The highest *FE* was around 87 % at -1.8 V vs. Ag/AgCl when 11.1
525 wt%. of PTFE was added, improving the *FE* to HOOCH to a value of 25.4 %. As can be
526 noticed in these studies, the type and concentration of the electrolytes have a great
527 influence on the maximum achieved *FE* that could be achieved. Besides, improvements
528 in the catalyst layer by adding different compounds are also an interesting approach.

529 Moreover, Alvarez-Guerra et al. [20] used a Pb plate as cathode and a solution of 0.45
530 M KHCO_3 + 0.5 M KCl as catholyte. The highest *FE* to HCOOH achieved was 94.7 %
531 at low current density values ($2.5 \text{ mA}\cdot\text{cm}^{-2}$) with a measured concentration of 14.4
532 $\text{mg}\cdot\text{L}^{-1}$. At the same conditions, a Sn plate was used as working electrode to compare
533 the performance of the process in terms of rate of HCOOH production and *FE* [24].
534 With a Sn cathode, the rates for HCOOH production were 25 % higher with efficiencies
535 around 70 %. Considering these results, Del Castillo et al. [40] applied GDEs loaded
536 with Sn particles with the aim of operating at higher *CD*. This Sn-GDE configuration
537 led to higher concentrations (885 and 1348 $\text{mg}\cdot\text{L}^{-1}$), maintaining an efficiency of about
538 70 %. One year later, Del Castillo et al. [63] analysed the effect of metal loading and
539 Sn-particle size in Sn-GDE electrodes in order to improve HCOOH formation rates. The
540 best results were observed with a catalytic loading of $0.75 \text{ mg Sn}\cdot\text{cm}^{-2}$ and a particle
541 size of 150 nm, achieving *FEs* around 70 % to HCOOH at $90 \text{ mA}\cdot\text{cm}^{-2}$, with rates and
542 concentration over $3.2 \text{ mmol}\cdot\text{m}^{-2} \text{ s}^{-1}$ and $1.5 \text{ g}\cdot\text{L}^{-1}$, respectively. They concluded that the
543 use of smaller Sn-NP (< 150 nm) and carbon supports for the electrochemical reduction
544 of CO_2 to HCOOH might allow further improvements in the process.

545 The utilisation of Pb-based catalyst as cathodes for the electroreduction of CO_2 to
546 HCOOH in L-L ecMRs has been also considered by Subramanian et al. [58], in which
547 the anode and the cathode chambers were separated by a composite perfluoro polymer
548 CEM. CO_2 was absorbed in a 0.2 M K_2HPO_4 + H_3PO_4 solution, which was fed to the
549 cathode chamber, obtaining a maximum *FE* to HCOOH of 93 % at $2 \text{ mA}\cdot\text{cm}^{-2}$. They
550 also showed that HCOOH concentration increases with *CD*. The highest measured
551 value was $0.016 \text{ mol}\cdot\text{L}^{-1}$ ($1085 \text{ mg}\cdot\text{L}^{-1}$), which is in the range of those concentrations
552 obtained by Del Castillo et al. [40] using DSA as anode. It should be remarked that the
553 utilisation of GDEs led to high *FE* when Sn and Pt are used as cathode and anode

554 catalysts, respectively. In order to analyse the viability of HCOOH production from
555 CO₂ electroreduction, Dominguez-Ramos et al. [74] studied the global warming
556 footprint associated to the process, identifying different scenarios and concluding that
557 the requirements of energy and materials are too high to ensure a sustainable production
558 of HCOOH from CO₂ electroreduction and thus, future technical advances are required.

559 In general, Sn-based catalysts allow obtaining HCOOH from CO₂ reduction with higher
560 *CDs* when compared to Pb-based catalyst, even though Sn-based catalysts have been
561 commonly used for this process, as found in literature. Besides, the modification of the
562 catalyst layer by adding different compounds, the utilisation of GDEs based on NPs and
563 alterations in the electrolyte may enhance the *FE* and concentration of HCOOH at the
564 reactor outlet.

565 *Pt-based electrodes*

566 In addition, Pt-based catalysts have been used for the electrochemical valorisation of
567 CO₂ in L-L ecMRs for DMC synthesis [30] and CO₂ electroreduction to HCOOH [25].
568 Garcia-Herrero et al. [30] used a Pt/Nb plate (95 % Pt) with 200 mL of CH₃OH in
569 combination with the ionic liquid [bmim][Br] and potassium methoxide as electrolyte.
570 A Nafion[®] 117 membrane was used. A concentration of 11.37 mM was achieved when
571 the electrolyte is formed by 80% CH₃OH, 15% ionic liquid and 5% CH₃OK. On the
572 other hand, Tamilarasan et al. [25] used a glassy carbon electrode with a Pt catalytic
573 loading of 1 mg cm⁻² at the cathode in a 0.5 M KHCO₃ solution. A polymer electrolyte
574 membrane was applied and the influence of operation mode in the cell (continuous or
575 discontinuous) was evaluated for HCOOH production at ambient conditions. The results
576 showed that higher concentrations can be obtained (almost double) in a continuous
577 operation mode (0 to 35 mmol·L⁻¹) in comparison to 18 mmol·L⁻¹ in a discontinuous
578 operation mode.

579 In conclusion, many researchers used CEMs, in particular Nafion[®] membranes, for the
580 electrochemical reduction of CO₂ in L-L ecMRs. Most of the anodes studied are based
581 on Pt plates. However, different catalyst materials and electrolytes at the cathode
582 compartment have been tested depending on the desired product. High *FES* to HCOOH
583 and CO have been achieved using CEMs, whereas further studies seems to be needed in
584 order to achieve higher *FE* and concentrations for the formation of hydrocarbons using
585 ecMRs.

586 4.1.2. L-L ecMRs based on AEMs

587 Materials based on Ag, Cu and Pt have been widely used as working electrodes for the
588 electrochemical reduction of CO₂ in order to obtain CO, hydrocarbons and DMC,
589 respectively, using AEMs in ecMRs. Besides, Pt has been commonly reported as anode
590 in these systems [19, 27, 36, 54, 68, 69].

591 Hatsukade et al. [19] studied the electrochemical reduction of CO₂ on silver surfaces. In
592 this work, an Ag foil was used as cathode, and an AEM was placed between the
593 electrodes to mitigate the transport of liquid products from the working to the counter
594 electrode. A solution of 0.1 M KHCO₃ was utilized as electrolyte (pH= 6.8 at the
595 catholyte) and a voltage range of -0.6 to -1.42 V vs. RHE was applied to the cell. CO
596 and H₂ were the main products obtained, with also HCOOH, CH₄, CH₃OH and
597 C₂H₅OH. The *FE* range for H₂, CO, HCOOH and other products formation were 10-100
598 %, 5-90 %, 2-8 % and < 0.1 %, respectively. A *FE*= 90 % to CO was achieved at -1.1 V
599 vs. RHE, whereas a *FE*= 8 % to HCOOH was obtained at -1.4 V vs. RHE.

600 Regarding Cu-based catalysts, Kuhl et al. [27] tested a Cu foil in order to analyse the
601 multicarbon products formed from CO₂ electroreduction, being 16 the different products
602 observed such as CH₄, C₂H₄ and HCOOH, together with ethylene glycol,

603 glycolaldehyde, hydroxyacetone, acetone or glyoxal, that are not commonly as CO₂
604 electroreduction products. A *FE* of 40 % to CH₄ was achieved at -1.15 V, whereas C₂H₄
605 and HCOOH were detected with a *FE* of 25 % at -1.05 V and 23 % *FE* at -0.87 V,
606 respectively. Besides, Chen et al. [54] applied different Cu-based catalysts (Cu
607 mesocrystals, Cu NP and electropolished Cu) for the electroreduction of CO₂ in an
608 aqueous solution of KHCO₃. The highest *FEs* were achieved when applying Cu
609 mesocrystals, with values of 27.2 %, 17.5 %, 7.5 % and 2.7 % for the production of
610 C₂H₄, HCOOH, CO and CH₄, respectively at different potentials.

611 In addition, Chen et al. [68] evaluated the influence of electrolyte conditions using
612 Cu₂O-derived Cu catalyst in order to electroreduce CO₂ to C₂H₆ in a three-electrode cell
613 with a 0.1 M KHCO₃ solution, when an AEM (SelemionTM) separated cathode and
614 anode compartments. The *FE* to C₂H₄ was 30 % at -1.2 V vs. Ag/AgCl, while traces of
615 C₂H₆ were observed. The other products obtained were H₂, HCOOH and alcohols.

616 Besides, adding PdCl₂ (100 mg) to the electrolyte at the same operation conditions,
617 produced increases in the *FE* to C₂H₆, with values of 30 % at -1.2 V vs. Ag/AgCl. They
618 proposed that C₂H₄ is firstly produced from CO₂ reduction at Cu sites. Afterwards, the
619 hydrogenation of C₂H₄ with the assistance of PdCl₂ occurs to produce C₂H₆. By
620 contrast, other Pd-based particles were also tested, but did not reach the same
621 conversion efficiencies. Ren et al. [69] also tested Cu₂O-based catalysts in an
622 electrochemical cell divided by an AEM in order to study the *FEs* to C₂H₄ and C₂H₅OH
623 in a 0.1 M KHCO₃ solution. In this way, Cu₂O layers deposited onto a Cu disc, and a Pt
624 wire were used as working and counter electrodes, respectively. The influence of the
625 Cu₂O layers was also discussed, concluding that 1.7-3.6 μm thickness led to the best *FE*
626 to C₂H₄ and C₂H₅OH at -1.2 V vs. Ag/AgCl, with values of 34-39 % and 9-16 %,
627 respectively. In these conditions, the *FE* to CH₄ was < 0.1 %. Therefore, it can be

628 concluded that the *FE* to C₂ products can be systematically tuned by varying the
629 thickness of Cu₂O overlayers.

630 As discussed in another section, Garcia-Herrero et al. [36] studied the influence of the
631 applied membrane in the electrochemical synthesis of DMC from CO₂. For this
632 purpose, an AEM and a Pt/Nb (95 % Pt) plate as working electrode was applied. The
633 maximum concentration achieved for DMC was 9.74 mmol·L⁻¹. The best results were
634 obtained without membrane in which the DMC concentration was 80.85 mmol·L⁻¹,
635 following by that concentration obtained when using a Nafion[®] CEM (11.37 mM). The
636 better performance in the absence of membrane was explained by mass transport
637 enhancements, although the presence of the ionic liquid [bmim][Br] was also required
638 to reach those values. Yim et al. [29] reached the same conclusion when no membrane
639 was applied in their system. In any case, the application of an undivided cell makes
640 difficult the separation of reaction products and thus, increases the cost associated to the
641 process.

642 Overall, the utilisation of AEMs rather than CEMs to divide the ecMR is gaining
643 importance due to the advantages of reducing polarization losses. Besides, high *FE* to
644 CO (90 %) has been achieved in Ag-based catalysts, which is comparable to the *FEs*
645 observed in some cases in which CEMs have been tested. Regarding the utilisation of
646 Cu-based catalysts, C₂H₄ has been obtained with Cu₂O and AEMs with acceptable *FEs*
647 (~ 30-40 %). Besides, C₂H₆ and C₂H₅OH have been also produced, where the thickness
648 of the Cu₂O layers seem to be critical in order to enhance efficiency.

649 As a result, further developments in terms of catalyst materials and electrolytes are
650 necessary to achieve the desired products with high *FEs*.

651 *4.2. Gas-Liquid (G-L) ecMRs*

652 Table 2 summarizes the different experimental conditions, catalytic materials, main
653 products and performance results for the use of G-L ecMRs in CO₂ electroreduction
654 processes. As for L-L ecMRs, CEMs are the common alternative to separate the
655 cathodic and the anodic compartments in these systems [11, 12, 17, 45, 46, 50, 52, 53,
656 55-57, 75, 76].

657 4.2.1. G-L ecMRs based on CEMs

658 Regarding the use of CEMs in G-L ecMRs, Delacourt et al. [11] used an integrated
659 system with a buffer layer between the Ag catalytic layer and the membrane for the
660 reduction of humidified CO₂. An enhanced selectivity for CO₂ reduction to CO was
661 observed, since the buffer layer probably prevented an excessive amount of protons
662 reaching the cathode. In fact, the *FE* to CO increases up to 80 % when a pH-buffer layer
663 of KHCO₃ was used. In addition, Wu et al. [50] studied the influence of a KHCO₃
664 buffer layer placed between the cathode and a Nafion[®] membrane in a G-L
665 configuration at pH= 7 when using a Sn-based GDEs. The onset potential for HCOOH
666 production was observed at -1.2 V and the *FE* was as high as 70 %. A high cell
667 potential was needed in order to overcome the anodic overpotential required for water
668 oxidation. It seems that buffer layers can be utilized to enhance the formation of CO and
669 HCOOH, increasing *FEs*. The pH and concentration of the buffer layer are also
670 essential to achieve high *FEs* in both systems.

671 Table 2. Experimental conditions, catalytic materials, main products and significant results for CO₂ valorisation in G-L ecMRs.

Membrane	Cathode	Anode	Catholyte	Anolyte	Products	V vs. Ag/AgCl / CD (mAcm ⁻²)	Main results	P (atm) / T (°C)	Ref.
Nafion®	Ag	Pt-Ir (1:1) alloy	Humidified CO ₂ gas	Pure water/KHC O ₃	CO, H ₂	-1.38 V	FE CO= 82 % with buffer layer	1 / 25	[11]
Sterion® (CEM)	Cu powders in carbon nanotubes (CNTs)	IrO ₂ over carbon paper	CO ₂ gas	H ₂ O saturated N ₂	C ₂ H ₄ O, methyl-HCOOH, CH ₄	-30 mA	Selectivity: C ₂ H ₄ O= 70 %; methyl-HCOOH= 13 %; CO= 10 %; CH ₄ = 7 %	1 / 90	[12]
Nafion® 117	Fe or Pt over CNTs	Pt wire	CO ₂ gas	aq. KCl	Alcohols and hydrocarbons (traces)	2 V	Fe-CNTs presents better performance	1 / 60	[17]
PEI and QPEI doped with KOH (AEM)	Cu ₂ O on porous carbon paper	Pt/C	CO ₂ gas	Deionized water	CO, H ₂ , CH ₄ , C ₂ H ₄ , C ₂ H ₆	* Cell potential: 1.8 to 3 V	FE CH ₄ = 6-11 %; C ₂ H ₄ = 3-20 %	1 / 25	[22]
Nafion® 115	Pt or Fe doped TPE-CMP/CNTs	Pt wire	CO ₂ gas	aq. KHCO ₃	C ₁ -C ₈ oxygenates.	-1.5 V	Highest productivity: 70 % Pt/TPE-CMP + 30 % CNTs (7.2x10 ⁻⁵ mmol·h ⁻¹).	- / 60	[45]
Nafion® 117	Metal NP on CNT/GDL	Pt wire	CO ₂ gas	aq. KCl	CO, H ₂ , CH ₃ OH, C ₂ H ₄ O, C ₂ H ₅ OH, acetone, C ₃ H ₈ O, CH ₃ COOH.	-	Fe-CNT/GDL: best productivity (4.8x10 ⁻⁴ mmol·h ⁻¹)	- / 25	[46]
Nafion® with buffer layer	Sn ink + GDL	Pt/C spray + GDL	CO ₂ gas	aq. KOH	HCOOH, CO, H ₂	-1.2 V	FE HCOOH= 70 %	1 / 25	[50]
AEM	Silver-coated	Pt plate	CO ₂ gas	aq. K ₂ SO ₄	CO, HCOOH, H ₂	-1.51 V / 20 mAcm ⁻²	FE CO= 92.1 %	1 / -	[51]
Nafion® 115	Cu foil	Pt flag	Humidified CO ₂ gas	aq. H ₂ SO ₄	CH ₄ , C ₂ H ₄	-1.95 V	FE CH ₄ = 8 %; C ₂ H ₄ = 10 %	- / 22	[52]
Nafion®	Cu-solid polymer electrolyte	Pt mesh	CO ₂ gas	aq. K ₂ SO ₄	CH ₄ , C ₂ H ₄ , CO, H ₂ , HCOOH	-1.45 V	FE H ₂ > 89 %	- / 22	[53]
Nafion®	Cu on porous carbon	Pt/C (40 % wt Pt)	CO ₂ gas	Alkali doped PVA	CH ₃ OH, HCOH, CH ₄	* Cell potential: 2 V	FE CH ₄ = 4.5 %; CH ₃ OH and HCOH < 1%	1 / 25	[55]
Glass frit	Sn-GDL	Pt wire	CO ₂ gas	aq. NaHCO ₃	HCOOH	-1.8 V	FE HCOOH= 70 %	-	[56]
AMI-7001	Cu ₂ O on porous	Pt/C (40%)	Humidified	water	CH ₄ , C ₂ H ₄ ,	-2.7 to -2.2 V	FE CH ₄ = 30 %; CH ₃ OH= 20	1 / 25	[57]

(AEM)	carbon paper	wt Pt)	CO ₂ gas		CH ₃ OH, H ₂		%; C ₂ H ₄ = 15 %		
Nafion [®]	TPE-CMP doped with metal NP	Pt wire	CO ₂ gas	aq. KHCO ₃	Hydrocarbons, C ₂ H ₄ O, H ₂ , alcohols	-	Hydrocarbon traces	- / 60	[75]
Nafion [®] 115	GDM-Fe metal doped	Pt wire	50 % CO ₂ in He	aq. KCl	CO, H ₂ , hydrocarbons and organics	10-20 mA	FE CO= 18.9 %; H ₂ = 80.6 %; hydrocarbons and organics= 0.55 %	- / 60	[76]

672

* Cell potential (not referred to any reference electrode)

673 Ampelli et al. [75] added different polymers to form Nafion-based MEAs with GDLs.
674 Different products such as CO, CH₃OH, C₂H₅OH, C₃H₈O, acetic acid and acetaldehyde
675 were obtained when Pt was supported on CNTs as electrocatalyst. The total *FE* was
676 higher than 95 % in all tests. Besides, the hydrocarbon and oxygenates production for
677 Pt-CNT with polymer (10 % weight metal) was also analysed. The results showed that
678 doping with an active metal is not enough to increase productivity, probably due to a
679 reduced conductivity. Nevertheless, small additions of CNT make possible to enhance
680 the productivity to an approximate value of 7×10^{-5} mmol.

681 Aeshala et al. [55] also used a Nafion[®] membrane to produce CH₄ in a G-L ecMR. Cu
682 was supported on carbon porous papers and a potential of 2 V was applied to the cell at
683 ambient conditions to reach a *FE* of about 4.5 %.

684 Genovese et al. [76] also studied the possibility of introducing another gas (He) into the
685 cathodic chamber together with CO₂ in a 50% concentration. A Nafion[®] 115 membrane
686 was used to form a GDE with the loaded metals (Fe or Pt). In these experiments, CO,
687 H₂, and hydrocarbons were observed, with the highest *FE* to CO achieved when the
688 metallic Fe catalyst was used (*FE*= 18.9 %). A Pt-based catalyst was also tested but the
689 *FE* to CO decreased. The *FE* to hydrocarbons was also less than 1 % in all cases. In this
690 regard, Genovese et al. [17] used a MEA composed of Fe or Pt electrocatalysts
691 supported on CNTs added to a Nafion[®] 117 membrane, while a Pt wire was used as
692 counter electrode, with the aim to obtain long C-chain products. The electrolyte utilized
693 at the anode side was a 0.5 M KCl solution. At 1 atm and 60 °C the Fe-CNTs
694 electrocatalysts presented better performance in terms of productivity of alcohols and
695 hydrocarbons at 2 V vs. Ag/AgCl. They concluded that both, the design of nanocarbon
696 materials and the correct evaluation of the engineering issues of electrodes and cells are

697 needed steps for the development of electrochemical processes for CO₂ reduction to
698 long-carbon chain products.

699 Ampelli et al. [46] used a Nafion[®] membrane and different metallic NP (Co, Cu, Fe and
700 Pt) supported over a functionalized CNT, forming a GDE for its use in G-L ecMRs. In
701 this case, CH₃OH, C₂H₅OH, C₃H₈O, acetaldehyde, acetone and some hydrocarbons
702 (C₄-C₉) were observed. When CO₂ in gas phase was used at the cathode, the
703 productivity was reduced in the following order: Fe-CNT > Fe-carbon black > Cu-CNT
704 > Pt-CNT. The highest productivity value achieved in the system was 4.8 x 10⁻⁴
705 mmol·h⁻¹ for Fe-CNT electrocatalysts. As previously mentioned, the absence of
706 electrolyte and the higher CO₂ concentration at the catalyst surface could inhibit the
707 mechanism of electron transfer, favouring the CO₂ dissociation to CO. Further reports
708 from Ampelli et al. [45] demonstrated the influence of different electrocatalysts for the
709 conversion of CO₂ to liquid fuels in gas-phase conditions using a tetrakis-phenylethene
710 conjugated microporous polymer (TPE-CMP) doped with Pt or Fe NP. Besides, CNTs
711 were also tested in combination with the previous catalysts with the aim to enhance
712 productivity. A Nafion[®] 115 membrane was assembled with the TPE-
713 CMP(CNTs)/GDL by hot-pressing method, forming the working electrode. The use of
714 CNTs in combination with the electrocatalysts (30 wt% CNTs) enhanced considerably
715 the performance due to a better dispersion of the ink onto the GDL and an enhanced
716 electrode conductivity [45]. The best result, in terms of C₁-C₈ oxygenates formation,
717 was 7.2 x 10⁻⁵ mmol·h⁻¹, when a 70 % Pt/TPE-CMP + 30 % CNTs was used as
718 electrocatalyst. This may show the potential use of CMPs for the process of CO₂
719 reduction in ecMRs.

720 Cu catalysts were also studied in G-L ecMRs using a Nafion[®] CEM in order to obtain
721 hydrocarbons from CO₂ [12, 52, 53]. Dewulf et al. [52] fed to the cathodic compartment

722 CO₂ humidified in an aqueous solution of KHCO₃. The obtained *FEs* ranged between 0-
723 8 % and 0-10 % to CH₄ and C₂H₄, respectively. The highest values were achieved for a
724 constant applied potential of -2 V.

725 As commented above, sandwiching the cathode, the membrane and the anode to form a
726 MEA for CO₂ reduction in gas phase makes possible to enhance CO₂ electroreduction.
727 In this sense, Gutiérrez-Guerra et al. [12] used a Cu powder-based MEA as cathode with
728 a hot-pressed Sterion[®] membrane (CEM) and IrO₂-carbon paper as anode. Water was
729 introduced into the anode side with N₂, while CO₂ in gas phase was used as catholyte.
730 Besides, electrocatalytic experiments were conducted at atmospheric pressure and in a
731 range of temperatures between 80 and 90 °C. CO₂ consumption rate was higher at 90 °C
732 in the different supports evaluated (i.e. graphite (G), activated carbon (AG) and carbon
733 nanofibers (CNF)). The product selectivity at the Cu-CNFs electrodes was C₂H₄O= 70
734 %, methyl-HCOOH= 13 %, CO= 10 %, CH₄= 7 % at -30 mA. The high selectivity for
735 C₂H₄O can be attributed to the size of Cu particle. In addition, Cu-AC electrodes
736 reached a selectivity of 50 % to C₂H₄O at -30 mA (with CH₃OH as the second main
737 product). However, Cu-G electrodes led to a higher selectivity to CH₃OH (75 %) at -30
738 mA. As a conclusion, an increase in *CD* for Cu-G and Cu-AC electrodes led to an
739 increase in CH₃OH selectivity due to the higher supplied rate of protons.

740 CH₄ and C₂H₄ were also obtained at Cu-based catalyst in a different report [77]. In this
741 case, different anolytes were applied (KOH, KHCO₃, KH₂PO₄ and K₂SO₄). The results
742 showed that the use of 1 M KOH led to the best performance when humidified CO₂ was
743 fed to the cathode. The maximum *FE* to C₂H₄ and CH₄ were 69 % and 9.1 %,
744 respectively, for an applied voltage of -2.72 V vs. Ag/AgCl. Conversely, Komatsu et al.
745 [53] used a dry CO₂ gas as reactant. In this case, C₂H₄, CH₄, CO, H₂ and HCOOH were
746 produced at 25 °C, although HER was predominant (*FE* about 89-97 %). They

747 concluded that the use of a CEM, with high protons transport capacity, is required for
748 the production of products that need high amounts of protons and electrons such as CH₄
749 and C₂H₄.

750 Prakash et al. [56] used a gas flow electrochemical cell, in which a glass frit was used to
751 separate the two compartments. A Sn-based cathode was applied for the production of
752 HCOOH, with a highest performance ($FE= 70\%$) found at -1.6 V vs. NHE.

753 As summary, different products such as CO, HCOOH, hydrocarbons and alcohols can
754 be achieved with high FEs from CO₂ electroreduction using CEM in G-L ecMRs. The
755 use of buffer layers between cathode and membrane seems to be an interesting approach
756 to increase the FE to CO and HCOOH in these reactors. Nevertheless, hydrocarbons
757 and alcohols have been obtained with poor FEs ($< 10\%$) and productivities, except for
758 the work developed by Cook et al. [77]. To overcome these limitations, the addition of
759 different microporous polymers into the membrane or the utilisation of CNTs as
760 catalytic support, among others, may be of help [45, 46]. These improvements may
761 probably lead to a better the near future.

762 4.2.2. G-L ecMRs based on AEMs

763 Other authors have tested AEMs for CO₂ electroreduction in G-L ecMRs [11, 22, 51,
764 57]. Delacourt et al. [11] employed an AEM (polyethersulfone-based membrane with
765 bicyclic ammonium groups) and humidified CO₂ as catholyte. In this case, a buffer
766 layer (KHCO₃) was not included in the reactor and the FE to CO (3 %) was
767 significantly lower than that obtained in configurations discussed above, in which a
768 buffer layer and a CEM (Nafion[®]) were used [11]. These authors also showed that the
769 use of AEM is advantageous when water is present at the anolyte because of the
770 generation of KHCO₃. Hori et al. [51] used Ag-coated AEM as electrode. The CEM

771 alone was not suitable for CO₂ reduction because the surface of the membrane was
772 partly ruptured during CO₂ reduction and the reaction was rapidly suppressed. Thus, the
773 use of an AEM allows a sustained reduction of CO₂ to CO, HCOOH and H₂ for more
774 than 2 h. The *FE* to CO was 92.1 % at 20 mA·cm⁻², whereas the *FE* to HCOOH was
775 12.1 % at 100 mA·cm⁻².

776 Aeshala et al. [22, 57] evaluated different membrane materials for the electrochemical
777 reduction of CO₂ in gas phase. In the first work [22] two different types of membrane
778 materials doped with KOH were used in order to prepare AEMs: polyethylenimine
779 (PEI) and quaternized PEI (QPEI). Besides, polyvinyl alcohol (PVA) was used as a
780 polymer matrix to form the membrane. The GDE was formed using Cu₂O particles
781 supported on porous carbon papers. H₂, CO, CH₄, C₂H₄ and C₂H₆ were the main
782 products obtained with a *FE* of 6-11 % CH₄ and 3-20 % to C₂H₆ and a product
783 selectivity of 67.6 % for C₂H₆ and 16.4 % for CH₄. In a second work [57], the same
784 authors evaluated a MEA configuration with CMI-7000 (CEM) and AMI-7001 (AEM)
785 at the same conditions for humidified CO₂ electroreduction. The results showed that the
786 performance for AMI-7001 membrane was more favourable than that for CMI-7000,
787 since the *FE* to interesting products were 30 % to CH₄, 15 % to C₂H₅OH and 20 % to
788 CH₃OH with AMI-7001 membrane, whereas CMI-7000 produced mainly H₂ (*FE*=
789 80%). That means that a correct membrane selection is essential to achieve high CO₂
790 electroreduction efficiencies.

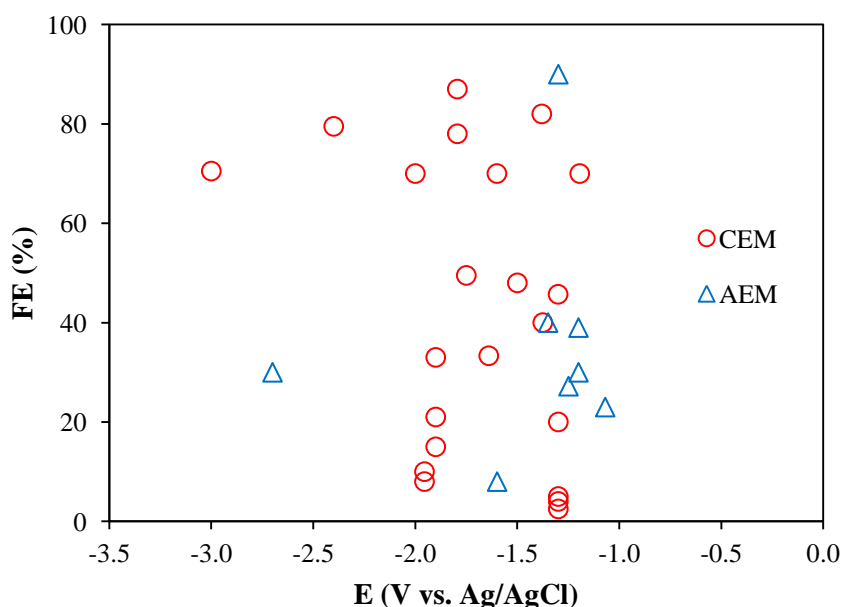
791 In general, the use of AEMs is considerably less efficient than using CEMs for the
792 electroreduction of CO₂ to CO (*FE*= 3 % vs. 82 %) as explained by Delacourt et al.
793 [11], even though Hori et al. [51] obtained higher *FE* to CO (92.1 %) using a Ag-coated
794 AEM as electrode at 20 mA·cm⁻². On the other hand, AEMs presented better
795 performance than CEMs for the production of hydrocarbons since CEMs favoured HER

796 instead of CO₂ reduction (*FE* ~ 80 % to H₂). Therefore, future research efforts should
797 also include the application of AEMs for the electrochemical reduction of CO₂.

798

799 4.3. Overview

800 Considering the crucial role of membranes in CO₂ reduction processes and the
801 considerable amount of studies reported, an overview of the *FEs* to different products
802 reached in the electrochemical reduction of CO₂ in L-L and G-L ecMRs at different *V* is
803 carried out. Figure 9 and Figure 10 show, respectively, the *FE* as a function of the
804 membrane applied and the main product obtained at different applied potentials vs.
805 Ag/AgCl. It should be noted that the figures uniquely provide a picture for the
806 comparison of different membrane materials, although the data come from studies
807 where different variables, namely cathode materials, products, reaction medium,
808 operating conditions and/or cell/electrode structure, may affect the results.

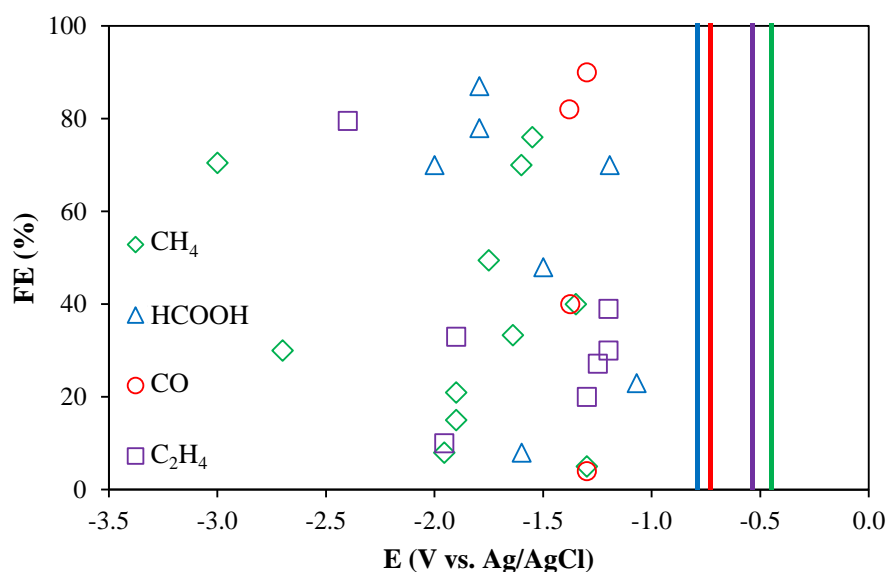


809

810 Figure 9. *FE* vs. *V* as a function of the type of membrane applied in L-L and G-L

811 ecMRs.

812 From the figure, it seems that the use of CEMs is, in general, more favourable to reach
 813 higher *FEs*. Although it also depends on the reduced products obtained, as shown in
 814 Figure 10. Additionally, the application of CEMs are more common than AEMs for the
 815 electrochemical valorisation of CO₂, although AEMs may lower polarization losses and
 816 thus their application may be an opportunity for high efficient CO₂ electroreduction
 817 systems.



818

819 Figure 10. *FE* vs. *V* for the formation of main products in L-L and G-L ecMRs. The
 820 points are experimental data and the lines are referred to the equilibrium potential for
 821 each product (HCOOH= -0.809 V; CO= -0.729 V; C₂H₄= -0.539 V; CH₄= -0.439 V vs.
 822 Ag/AgCl).

823 Unsurprisingly, the best *FEs* were obtained for CO and HCOOH formation. The highest
 824 *FE* to CO (~ 90-100 %) was achieved using L-L ecMRs [19, 49] and a G-L ecMR [51]
 825 with Ag-based catalysts at the cathode side. Hatsukade et al. [19] achieved a *FE*= 90 %
 826 at -1.3 V vs. Ag/AgCl using a Ag-Foil as working electrode in an electrochemical
 827 reactor divided by an AEM. Besides, Rosen et al. [49] obtained a *FE* to CO near to 100

828 % by adding 89.5 % mol of water to the ionic liquid [bmim][BF₄] as electrolyte in a L-L
829 ecMR divided by a CEM, where Ag NP were used as electrocatalyst. Additionally, a
830 similar *FE* was achieved by Hori et al. [51], who reported a *FE* to CO= 92.1 % at -1.51
831 V vs. Ag/AgCl with a Ag-coated electrode in a G-L ecMR divided by an AEM.

832 On the other hand, the best *FEs* to HCOOH (~ 90 %) were achieved in L-L ecMRs with
833 Sn-GDEs electrodes [10, 43] and CEMs at 50 mA·cm⁻² and -1.8 V vs. Ag/AgCl,
834 respectively, even though Pb plates also allowed to obtain similar *FEs* at low *CD* [20,
835 58]. In addition, high concentrations of HCOOH (~ 1.5 g·L⁻¹) were achieved in Sn-GDE
836 electrodes with smaller *FE* (70 % at -2 V and 90 mA·cm⁻²) by Del Castillo et al. [63].

837 Regarding hydrocarbon formation, the highest *FEs* to CH₄ and to C₂H₄ were 76 % at -
838 1.55 V vs. Ag/AgCl and 79.5 % at -2.4 V vs. Ag/AgCl, respectively, in L-L ecMRs
839 [35, 64]. In these studies, Cu-based electrocatalysts were applied in combination with
840 CEMs in divided cells. However, other available reports did not show *FEs* higher than
841 50 % and 30 % in L-L and G-L ecMRs, respectively (considerably lower than *FEs*
842 obtained to CO and HCOOH in these reactors). Therefore, the development of novel
843 approaches in terms of reactor configuration, catalyst materials and electrolyte
844 composition, among others, should be considered in the future in order to obtain
845 hydrocarbons with high *FEs* and *CDs* in ecMRs.

846 Moreover, a deeper characterization of the reaction mechanism by which products are
847 formed is crucial to design effective electrocatalysts for the electrochemical reduction of
848 CO₂ [78]. Unfortunately, the different mechanisms of products obtained on different
849 catalysts are still unclear. Different intermediates have been identified in the literature
850 on dependence of the CO₂ reduction pathway. In this regard, CO₂⁻_{ads}, CO_{ads}, HCO_{ads}[·]
851 and H₃CO_{ads}[·] have been proposed to be probable intermediates in the electrochemical
852 reduction of CO₂ to HCOOH, CO, CH₄ and CH₃OH, respectively. Besides, Kortlever et

853 al. [79] argue that the electrolyte composition and the pH may change the results of the
854 reaction significantly. Besides, they also considered that the absorbed CO_2^- anion
855 intermediate and the absorbed $(\text{CO})_2^-$ anionic dimer play an essential role in some of
856 mechanistic pathways for C1 and C2 production, even though the electrocatalyst, the
857 electrolyte and the operating conditions applied also affect in the pathways for the
858 electrochemical reduction of CO_2 . Therefore, the optimal electroreduction of CO_2
859 requires catalysts with suitable absorption properties and electrolytes with positive
860 impacts on the catalytic selectivity and activity [79].

861 Finally, the highly endothermic CO_2 conversion reactions consume lots of energy.
862 Therefore, the high costs associated to these processes should be considered. In this
863 regard, the use of renewable energy might be of help in order to achieve an
864 economically viable CO_2 electroreduction process. It seems that further efforts on
865 evaluating the whole life cycle of CO_2 conversion processes are required.

866

867 **4. Conclusions and future prospects**

868 In this review, studies on CO_2 electroreduction in different membrane reactor
869 configurations have been compiled and discussed in terms of type of membrane applied,
870 electrode configuration and electrocatalyst applied in order to analyse the different
871 technical solutions to perform the electrochemical reduction of CO_2 into valuable
872 products using electrochemical membrane reactors. The role of membranes in these
873 reactors is to divide the cathode and anode compartments, improving the separation of
874 products and avoiding their re-oxidation. Besides, GDEs can be coupled with ionic
875 exchange membranes (cation or anion) with the aim to form membrane electrode
876 assemblies (MEAs). These systems reduce mass transfer limitations and increase

877 process efficiency, and are gaining importance in CO₂ electrochemical reduction
878 processes. Nafion[®] membranes are the most common membranes applied, especially
879 when high amounts of protons are necessary to form more reduced species. Liquid-
880 Liquid electrochemical membrane cells are the most studied reactors. Gas-Gas ecMRs
881 reports, however, are recently emerging due to the mass transport enhancements at both,
882 cathode and anode compartments. Furthermore, different metal-based catalysts such as
883 silver, copper, tin and lead are used as electrocatalysts for CO₂ valorisation into
884 different products, such as carbon monoxide, hydrocarbons and formic acid,
885 respectively in aqueous salt solutions such as Na⁺, K⁺, Cl⁻, HCO₃⁻ and OH⁻.

886 As a conclusion, further advances in new reactor configuration, membranes and
887 catalytic materials need to be accomplished before achieving high conversion rates, *FES*
888 and *CDs* for the electrochemical reduction of CO₂ in ecMRs.

889 In this regard, the authors recommend to focus the research efforts on the:

890 i) development of reactor configurations based on GDEs and MEAs, which favour the
891 transport of components; ii) addition of new polymers in ion exchange membranes, in
892 order to improve the electrode conductivity; iii) development of new highly active
893 nanostructured materials as catalyst support, which are able to increase the productivity
894 for the desired products; iv) study of different electrolyte solutions, including also ionic
895 liquids with the aim of suppressing HER; and v) identify favourable operating
896 conditions (i.e. pressure, temperature, *V*, *CD*, and CO₂ flow rates) for an enhanced
897 reduction of CO₂ in continuous operation.

898

899 **Acknowledgements**

900 The authors gratefully acknowledge the financial support of the Spanish Ministry of
901 Economy and Competitiveness (MINECO) through the project CTQ2013-48280-C3-1-
902 R. Ivan Merino-Garcia and Jonathan Albo would like to thank the MINECO for the
903 Early Stage Researcher grant (BES2014-070081) and *Juan de la Cierva* postdoctoral
904 program (JCI-2012-12073).

905

906 **References**

907 [1] Intergovernmental panel on climate change (2014). Climate change 2014: Mitigation
908 of climate change. 12th session of IPCC WG III, Berlin, Germany (7-11 April 2014)

909 [2] J. Albo, A. Irabien, Non-dispersive absorption of CO₂ in parallel and cross-flow
910 membrane modules using EMISE, J. Chem. Technol. Biot. 87:10 (2012) 1502-1507.

911 [3] G. Centi and S. Perathoner, Opportunities and prospects in the chemical recycling of
912 carbon dioxide to fuels, Catal. Today 148 (2008) 191-205.

913 [4] K. S. Lackner, Carbonate chemistry for sequestering fossil carbon, Annu. Rev.
914 Energy Environ. 27 (2002) 193-232.

915 [5] D. T. Whipple and P. J. A. Kenis, Prospects of CO₂ utilization via direct
916 heterogeneous electrochemical reduction, J. Phys. Chem. Lett. 1 (2010) 3451-3458.

917 [6] H. R. M. Jhong, S. Ma, P. J. A. Kenis, Electrochemical conversion of CO₂ to useful
918 chemicals: current status, remaining challenges, and future opportunities, Curr. Opin.
919 Chem. Eng. 2 (2013) 191-199.

920 [7] B. Hu, C. Guild, S. L. Suib, Thermal, electrochemical, and photochemical
921 conversion of CO₂ to fuels and value-added products, J. CO₂ Util. 1 (2013) 18-27.

- 922 [8] J. P. Jones, G. K. S. Prakash, G. A. Olah, Electrochemical CO₂ reduction: recent
923 advances and current trends, *Isr. J. Chem.* 53 (2013) 1-17.
- 924 [9] E. V. Kondratenko, G. Mul, J. Baltrusaitis, G. O. Larrazabal, J. Perez-Ramirez,
925 Status and perspectives of CO₂ conversion into fuels and chemicals by catalytic,
926 photocatalytic, and electrocatalytic processes, *Energy Environ.* 6 (2013) 3112-3135.
- 927 [10] D. Kopljär, A. Inan, P. Vindayer, N. Wagner, E. Klemm, Electrochemical
928 reduction of CO₂ to formate at high current density using gas diffusion electrodes, *J.*
929 *Appl. Electrochem.* 44 (2014) 1107-1116.
- 930 [11] C. Delacourt, P.L. Ridgway, J.B. Kerr, J. Newman, Design of an electrochemical
931 cell making syngas (CO + H₂) from CO₂ and H₂O reduction at room temperature, *J.*
932 *Electrochem. Soc.* 155 (2008) B42-B49.
- 933 [12] N. Gutiérrez-Guerra, L. Moreno-López, J. C. Serrano-Ruiz, J. L. Valverde, A. de
934 Lucas-Consuegra, Gas phase electrocatalytic conversion of CO₂ to syn-fuels on Cu
935 based catalysts-electrodes, *Appl. Catal. B-Environ.* 188 (2016) 272-282.
- 936 [13] R. L. Cook, R. C. Macduff, A. F. Sammells, Ambient temperature gas phase CO₂
937 reduction to hydrocarbons at solid polymer electrolyte cells, *J. Electrochem. Soc.* 135
938 (1988) 1470-1471.
- 939 [14] S.M.A. Kriescher, K. Kugler, S.S. Hosseiny, Y. Gendel, M. Wessling, A
940 membrane electrode assembly for the electrochemical synthesis of hydrocarbons from
941 CO_{2(g)} and H_{2O(g)}, *Electrochem. Commun.* 50 (2015) 64-68.
- 942 [15] R. J. Lim, M. Xie, M. A. Sk, J. M. Lee, A. Fisher, X. Wang, K. H. Lim, A review
943 on the electrochemical reduction of CO₂ in fuel cells, metal electrodes and molecular
944 catalyst, *Catal. Today* 233 (2014) 169-180.

- 945 [16] Y. Oh and X. Hu, Organic molecules as mediators and catalysts for photocatalytic
946 and electrocatalytic CO₂ reduction, *Chem. Soc. Rev.* 42 (2013) 2253-2261.
- 947 [17] C. Genovese, C. Ampelli, S. Perathoner, G. Centi, Electrocatalytic conversion of
948 CO₂ to liquid fuels using nanocarbon-based electrodes, *J. Energ. Chem.* 22 (2013) 202-
949 213.
- 950 [18] J. Qiao, Y. Liu, F. Hong, J. Zhang, A review of catalyst for the electroreduction of
951 carbon dioxide to produce low-carbon fuels, *Chem. Soc. Rev.* 43 (2014) 631-675.
- 952 [19] T. Hatsukade, K.P Kuhl, E.R. Cave, D.N. Abram, T.F. Jaramillo, Insights into the
953 electrocatalytic reduction of CO₂ on metallic silver surfaces, *Phys. Chem. Chem. Phys.*
954 16 (2014) 13814-13819.
- 955 [20] M. Alvarez-Guerra, S. Quintanilla, A. Irabien, Conversion of carbon dioxide into
956 formate using a continuous electrochemical reduction process in a lead cathode, *Chem.*
957 *Eng. J.* 207-208 (2012) 278-284.
- 958 [21] J. Albo, A. Sáez, J. Solla-Gullón, V. Montiel, A. Irabien, Production of methanol
959 from CO₂ electroreduction at Cu₂O and Cu₂O/ZnO-based electrodes in aqueous
960 solution, *Appl. Catal. B-Environ.* 176-177 (2015) 709-717.
- 961 [22] L. M. Aeshala, R. Uppaluri, A. Verma, Electrochemical conversion of CO₂ to
962 fuels: tuning the reaction zone using suitable functional groups in solid polymer
963 electrolyte, *Phys. Chem. Chem. Phys.* (2014). DOI: 10.1039/c0xx00000x.
- 964 [23] H. Li, C. Oloman, The electro-reduction of carbon dioxide in a continuous reactor,
965 *J. Appl. Electrochem.* 35 (2005) 955-965.

966 [24] M. Alvarez-Guerra, A. Del Castillo, A. Irabien, Continuous electrochemical
967 reduction of carbon dioxide into formate using a tin cathode: Comparison with lead
968 cathode, *Chem. Eng. Res. Des.* 92 (2014) 692-701.

969 [25] P. Tamilarasan, S. Ramaprabhu, Task-specific functionalization of graphene for
970 cathode catalyst support in carbon dioxide conversion, *Journal of Materials Chemistry*
971 *A* (2014) 1-27.

972 [26] S. Kaneco, K. Iiba, S.K. Suzuki, K. Ohta, T. Mizuno, Electrochemical reduction of
973 carbon dioxide to hydrocarbons with high Faradaic efficiency in LiOH/Methanol, *J.*
974 *Phys. Chem. B* 103 (1999) 7456-7460.

975 [27] K.P. Kuhl, E.R. Cave, D.N. Abram, T.F. Jaramillo, New insights into the
976 electrochemical reduction of carbon dioxide on metallic copper surfaces, *Energ.*
977 *Environ. Sci.* 5 (2012) 7050-7059.

978 [28] R. Kas, R. Kortlever, A. Milbrat, M. T. M. Koper, G. Mul, J. Baltrusaitis,
979 Electrochemical CO₂ reduction on Cu₂O-derived copper nanoparticles: controlling the
980 catalytic selectivity of hydrocarbons, *Phys. Chem. Chem. Phys.* 16 (2014) 12194-
981 12201.

982 [29] K. J. Yim, D. K. Song, C. S. Kim, N. G. Kim, T. Iwaki, T. Ogi, K. Okuyama, S. E.
983 Lee, T. O. Kim, Selective, high efficiency reduction of CO₂ in a non-diaphragm-based
984 electrochemical system at low applied voltage, *RSC. Adv.* 00 (2014) 1-3.

985 [30] I. Garcia-Herrero, M. Alvarez-Guerra, A. Irabien, CO₂ electro-valorisation to
986 dimethyl carbonate from methanol using potassium methoxide and the ionic liquid
987 [bmim][Br] in a filter-press electrochemical cell, *J. Chem. Technol. Biotechnol.* 90
988 (2015) 1433-1438.

- 989 [31] M. R. Gonçalves, A. Gomes, J. Condeço, R. Fernandes, T. Pardal, C. A. C.
990 Sequeira, J. B. Branco, Selective electrochemical conversion of CO₂ to C₂
991 hydrocarbons, *Energ. Convers. Manage.* 51 (2010) 30-32.
- 992 [32] M. R. Gonçalves, A. Gomes, J. Condeço, R. Fernandes, T. Pardal, C. A. C.
993 Sequeira, J. B. Branco, Electrochemical conversión of CO₂ to C₂ hydrocarbons using
994 different ex situ copper electrodeposits, *Electrochim. Acta* 102 (2013) 388-392.
- 995 [33] S. Kaneco, H. Katsumata, T. Suzuki, K. Ohta, Electrochemical reduction of CO₂ to
996 methane at the Cu electrode in methanol with sodium supporting salts and it's
997 comparison with other alkaline salts, *Energy & Fuels* 20 (2006) 409-414.
- 998 [34] R. Aydin, H. O. Dogan, F. Köleli, Electrochemical reduction of carbon dioxide on
999 polypyrrole coated copper electro-catalyst under ambient and high pressure in methanol,
1000 *Applied Catalysis B* 140-141 (2013) 478-482.
- 1001 [35] H. Yano, T. Tanaka, M. Nakayama, K. Ogura, Selective electrochemical reduction
1002 of CO₂ to ethylene at a three phase interface on copper (I) halide-confined Cu-mesh
1003 electrodes in acidic solutions of potassium halides, *Journal of Electroanalytical*
1004 *Chemistry* 565 (2004) 287-293.
- 1005 [36] I. Garcia-Herrero, M. Alvarez-Guerra, A. Irabien, Electrosynthesis of dimethyl
1006 carbonate from methanol and CO₂ using potassium methoxide and the ionic liquid
1007 [bmim][Br] in a filter-press cell: a study of the influence of cell configuration, *J. Chem.*
1008 *Technol. Biotechnol.* 91:2 (2016) 507-513.
- 1009 [37] C. Genovese, C. Ampelli, S. Perathoner, G. Centi, Electrocatalytic conversion of
1010 CO₂ to liquid fuels using nanocarbon-based electrodes, *J. Energy Chem.* 22 (2013) 202-
1011 213.

1012 [38] M. R. Singh, E. L. Clark, A. T. Bell, Effects of electrolyte, catalyst, and membrane
1013 composition and operating conditions on the performance of solar-driven
1014 electrochemical reduction of carbon dioxide, *Phys. Chem. Chem. Phys.* 17 (2015) 18924-
1015 18936.

1016 [39] C. Genovese, C. Ampelli, S. Perathoner, G. Centi, A gas-phase electrochemical
1017 reactor for carbon dioxide reduction back to liquid fuels, *Chem. Eng. Trans.* 32 (2013)
1018 289-294.

1019 [40] A. Del Castillo, M. Alvarez-Guerra, A. Irabien, Continuous electroreduction of
1020 CO₂ to formate using Sn gas diffusion electrodes, *AIChE J.* 60 (2014) 3557-3564

1021 [41] Q. Wang, H. Dong, H. Yu, Development of rolling tin gas diffusion electrode for
1022 carbon dioxide electrochemical reduction to produce formate in aqueous electrolyte, *J.*
1023 *Power Sources* 271 (2014) 278-284.

1024 [42] H. Yano, F. Shirai, M. Nakayama, K. Ogura, Electrochemical reduction of CO₂ at
1025 three phase (gas/liquid/solid) and two phase (liquid/solid) interfaces on Ag electrodes, *J.*
1026 *Electroanal. Chem.* 533 (2002) 113-118.

1027 [43] Q. Wang, H. Dong, H. Yu, H. Yu, Enhanced performance of gas diffusion
1028 electrode for electrochemical reduction of carbon dioxide to formate by adding
1029 polytetrafluoroethylene into catalyst layer, *J. Power Sources* 279 (2015) 1-5.

1030 [44] J. Albo, A. Irabien, Cu₂O-loaded gas diffusion electrodes for the continuous
1031 electrochemical reduction of CO₂ to methanol, *J. Catal.* (2015),
1032 <http://dx.doi.org/10.1016/j.jcat.2015.11.014>

1033 [45] C. Ampelli, C. Genovese, M. Errahali, G. Gatti, L. Marchese, S. Perathoner, G.
1034 Centi, CO₂ capture and reduction to liquid fuels in a novel electrochemical setup by

1035 using metal-doped conjugated microporous polymers, *J. Appl. Electrochem.* 45 (2015)
1036 701-713.

1037 [46] C. Ampelli, C. Genovese, B. C. Marepally, G. Papanikolaou, S. Perathoner, G.
1038 Centi, Electrocatalytic conversion of CO₂ to produce solar fuels in electrolyte or
1039 electrolyte-less configurations of PEC cells, *Faraday Discuss.* 00 (2015) 1-3.

1040 [47] B. A. Rosen, A. Salehi-Khojin, M. R. Thorson, W. Zhu, D. T. Whipple, P. J. A.
1041 Kenis, R. I. Masel, Ionic Liquid-mediated selective conversion of CO₂ to CO at low
1042 overpotentials, *Science Express* 334 (2011) 643-644.

1043 [48] A. Salehi-Khojin, H. R. M. Jhong, B. A. Rosen, W. Zhu, S. Ma, P. J. A. Kenis, R.
1044 I. Masel, Nanoparticle silver catalyst that show enhanced activity for carbon dioxide
1045 electrolysis, *J. Phys. Chem. C* 117 (2013) 1627-1632.

1046 [49] B. A. Rosen, W. Zhu, G. Kaul, A. Salehi-Khojin, R. I. Masel, Water enhancement
1047 of CO₂ conversion on silver in 1-ethyl-3-methylimidazolium tetrafluoroborate, *J.*
1048 *Electrochem. Soc.* 160 (2013) H138-H141.

1049 [50] J. Wu, F.G. Risalvato, P.P. Sharma, P.J. Pellechia, F.S. Ke, X.D. Zhou,
1050 Electrochemical reduction of carbon dioxide II. Design, assembly, and performance of
1051 low temperature full electrochemical cells, *J. Electrochem. Soc.* 160 (2013) F953-F957.

1052 [51] Y. Hori, H. Ito, K. Okano, N. Nagasu, S. Sato, Silver-coated ion exchange
1053 membrane electrode applied to electrochemical reduction of carbon dioxide,
1054 *Electrochim. Acta* 48 (2003) 2651-2657.

1055 [52] D. W. Dewulf, A. J. Bard, The electrochemical reduction of CO₂ to CH₄ and C₂H₄
1056 at Cu/Nafion electrodes (solid polymer electrolyte structures), *Catalysis Letters* 1 (1988)
1057 73-80.

- 1058 [53] S. Komatsu, M. Tanaka, A. Okumura, A. Kungi, Preparation of Cu-solid polymer
1059 electrolyte composite electrodes and applications to gas-phase electrochemical
1060 reduction of CO₂, *Electrochimica Acta* 40 (1995) 745-753.
- 1061 [54] C. S. Chen, A. D. Handoko, J. H. Wan, L. Ma, D. Ren, B. S. Yeo, Stable and
1062 selective electrochemical reduction of carbon dioxide to ethylene on copper
1063 mesocrystals, *Catal. Sci. Technol.* 5 (2014) 161-168.
- 1064 [55] L. M. Aeshala, S. U. Rahman, A. Verma, Effect of solid polymer electrolyte on
1065 electrochemical reduction of CO₂, *Separation and Purification Technology* 94 (2012)
1066 131-137.
- 1067 [56] G. K. S. Prakash, F. A. Viva, G. A. Olah, Electrochemical reduction of CO₂ over
1068 Sn-Nafion coated electrode for a fuel-cell-like device, *J. Power Sources* 223 (2013) 68-
1069 73.
- 1070 [57] L. M. Aeshala, R. Uppaluri, A. Verma, Effect of cation and anion solid polymer
1071 electrolyte on direct electrochemical reduction of gaseous CO₂ to fuel, *Journal of CO₂*
1072 *utilisation* 3-4 (2013) 49-55.
- 1073 [58] K. Subramanian, K. Asokan, D. Jeevarathinam, M. Chandrasekaran,
1074 Electrochemical membrane reactor for the reduction of carbon dioxide to formate, *J.*
1075 *Appl. Electrochem.* 37 (2007) 255-260.
- 1076 [59] S. Singh, C. Mukherjee, A. Verma, Development of catalytic activity protocol for
1077 electrochemical reduction of carbon dioxide to value added products, *Clean Techn.*
1078 *Environ. Policy* 17 (2015) 533-540.

1079 [60] J. Xie, Y. Huang, H. Yu, Tuning the catalytic selectivity in electrochemical CO₂
1080 reduction on copper oxide-derived nanomaterials, *Front. Environ. Sci. Eng.* (2014).
1081 DOI: 10.1007/s11783-014-0742-1.

1082 [61] Y. Hori, H. Wakebe, T. Tsukamoto, O. Koga, Electrocatalytic process of CO
1083 selectivity in electrochemical reduction of CO₂ at metal electrodes in aqueous media,
1084 *Electrochim. Acta* 39 (1994) 1833-1839.

1085 [62] Y. Hori, H. Wakebe, T. Tsukamoto, O. Koga, Adsorption of CO accompanied with
1086 simultaneous charge transfer on copper single crystal electrodes related with
1087 electrochemical reduction of CO₂ to hydrocarbons, *Surface Science* 335 (1995) 258-
1088 263.

1089 [63] A. Del Castillo, M. Alvarez-Guerra, J. Solla-Gullón, A. Sáez, V. Montiel, A.
1090 Irabien, Electrocatalytic reduction of CO₂ to formate using particulate Sn electrodes:
1091 effect of metal loading and particle size, *Appl. Energ.* 157 (2015) 165-173.

1092 [64] K. Manthiram, B. J. Beberwyck, A. P. Alivisatos, Enhanced electrochemical
1093 methanation of carbon dioxide with a dispersible nanoscale copper catalyst, *J. Am.*
1094 *Chem. Soc.* 136 (2014) 13319-13325.

1095 [65] R. Kas, R. Kortlever, H. Yilmaz, M. T. M. Koper, G. Mul, Manipulating the
1096 hydrocarbon selectivity of copper nanoparticles in CO₂ electroreduction by process
1097 conditions, *ChemElectroChem* 2 (2015) 354-358.

1098 [66] A. S. Varela, M. Kroschel, T. Reier, P. Strasser, Controlling the selectivity of CO₂
1099 electroreduction on copper: the effect of the electrolyte concentration and the
1100 importance of the local pH, *Catal. Today* 260 (2016) 8-13.

- 1101 [67] C. Genovese, C. Ampelli, B. C. Marepally, G. Papanikolaou, S. Perathoner, G.
1102 Centi, Electrocatalytic reduction of CO₂ for the production of fuels: a comparison
1103 between liquid and gas phase condition, *Chem. Eng. Trans.* 43 (2015) 2281-2286.
- 1104 [68] C. S. Chen, J. H. Wan, B. S. Yeo, Electrochemical reduction of carbon dioxide to
1105 ethane using nanostructured Cu₂O-derived copper catalyst and palladium(II) chloride, *J.*
1106 *Phys. Chem. C* 119 (2015) 26875-26882.
- 1107 [69] D. Ren, Y. Deng, A. D. Handoko, C. S. Chen, S. Malkhandi, B. S. Yeo, Selective
1108 electrochemical reduction of carbon dioxide to ethylene and ethanol on copper(I) oxide
1109 catalysts, *ACS Catal.* 5 (2015) 2814-2821.
- 1110 [70] M. Alvarez-Guerra, J. Albo, E. Alvarez-Guerra, A. Irabien, Ionic liquids in the
1111 electrochemical valorisation of CO₂, *Energy Environ. Sci.* 8(2015)2574-2599.
- 1112 [71] K. Ogura, M. D. Salazar-Villalpando, CO₂ electrochemical reduction via adsorbed
1113 halide anions, *Energy Conservation* 63 (2011) 35-38.
- 1114 [72] G. Keerthiga, B. Viswanathan, R. Chetty, Electrochemical reduction of CO₂ on
1115 electrodeposited Cu electrodes crystalline phase sensitivity on selectivity, *Catal. Today*
1116 245 (2015) 68-73.
- 1117 [73] J. Albo, M. Alvarez-Guerra, P. Castaño, A. Irabien, Towards the electrochemical
1118 conversion of carbon dioxide into methanol, *Green Chem.* 17 (2015) 2304-2324.
- 1119 [74] A. Dominguez-Ramos, B. Singh, X. Zhang, I.E. Hertwich, A. Irabien, Global
1120 warming footprint of the electrochemical reduction of carbon dioxide to formate, *J.*
1121 *Clean. Prod.* 148 (2015) 148-155.

- 1122 [75] C. Ampelli, C. Genovese, S. Perathoner, G. Centi, M. Errahali, G. Gatti, L.
1123 Marchese, An electrochemical reactor for the CO₂ reduction in gas phase by using
1124 conductive polymer based electrocatalysts, *Chem. Eng. Trans.* 41 (2014) 13-18.
- 1125 [76] C. Genovese, C. Ampelli, S. Perathoner, G. Centi, Electrocatalytic conversion of
1126 CO₂ on carbon nanotube-based electrodes for producing solar fuels, *Journal of Catalysis*
1127 308 (2013) 237-249.
- 1128 [77] R. L. Cook, R. C. Macduff, A. F. Sammells, High rate gas phase CO₂ reduction to
1129 ethylene and methane using gas diffusion electrodes, *J. Electrochem. Soc.* 137 (1990)
1130 607-608.
- 1131 [78] D. Ren, Y. Huang, B. S. Yeo, Electrocatalysts for the selective reduction of carbon
1132 dioxide to useful products, *Chimia* 69 (2015) 131-135.
- 1133 [79] R. Kortlever, J. Shen, K. P. Schouten, F. Calle-Vallejo, M. T. M. Koper, Catalyst
1134 and reaction pathways for the electrochemical reduction of carbon dioxide, *J. Phys.*
1135 *Chem. Lett.* 6 (2015) 4073-4082.

Table 1

Table 1. Experimental conditions, materials, main products and significant results of the Liquid-Liquid electrochemical membrane reactors.

Ref.	T (°C)	Pressure (atm)	Membrane	Cathode	Anode	Catholyte	Anolyte	Reference electrode	Products	Main results
9	25	1	Nafion [®]	Ag	Pt-Ir (1:1) alloy	CO ₂ , KHCO ₃	Aq. KOH	SCE	CO, H ₂	40 % FE CO at -1.42 V and 20 mA/cm ²
19	---	---	Selemion [™] (anion)	Cu foil	Pt foil	CO ₂ , KHCO ₃	Aq. KHCO ₃	Ag/AgCl (converted to RHE)	16 different products	FE: 40 % methane at -1.15 V, 25 % ethylene at -1.05 V, 23% formate at -0.87 V
20	25	1	Selemion [™] (anion)	Ag foil	Pt foil	CO ₂ , KHCO ₃	Aq. KHCO ₃	RHE	CO, H ₂ , formate, methane, methanol, ethanol	90 % FE CO at -1.1 V and 8% FE formate at -1.4 V
21	25	1	Nafion [®] 450	Mesh tinned-copper plate	platinized titanium plate	CO ₂ y N ₂ , KHCO ₃	Aq. KOH	SHE	Formate, H ₂ , CO, methane	86 % FE formate at 22 mA/cm ²
22	25	1	Nafion [®] 117	Pb plate	DSA	CO ₂ , KCl + KHCO ₃	Aq. KOH	Ag/AgCl	Formate	14.4 mg/L and 94.7 % FE to formate at 2.5 mA/cm ²
23	25	1	Nafion [®] 117	Sn plate	DSA	CO ₂ , KCl + KHCO ₃	Aq. KOH	Ag/AgCl	Formate	Formate FE about 70 % at 12.25 mA/cm ²
24	25	1	Nafion [®] 112	Cuprous oxide films electrodeposited onto copper plates	Pt mesh	CO ₂ , KHCO ₃	Aq. KHCO ₃	RHE	Ethane, ethylene, methane, CO	FE: 0-4 % CO, 1-5 % CH ₄ , 20 % C ₂ H ₄ , 2.5 % C ₂ H ₆ at -1.1 V
25	25	1.2	Nafion [®] 117 or no membrane	Cu insoluble plate	Pt insoluble plate	CO ₂ , NaOH or KOH in methanol	NaOH or KOH in methanol	---	Methane, H ₂	Without membrane and using KOH: 35.6 % FE to methane at 0.5 V
26	---	---	Nafion [®] 117	Pt/Nb plate (95% Pt)	Pt/Nb plate (95% Pt)	CO ₂ , methanol + [bmim][Br] + CH ₃ OK	Methanol + [bmim][Br] + CH ₃ OK	Ag/AgCl	Dimethyl carbonate	11.37 mmol/L of dimethyl carbonate
27	25	1	Cation ex. membrane	Cu mesh/modified copper electrodes	Pt mesh	CO ₂ , KHCO ₃	Aq. KHCO ₃	Ag/AgCl	Methane, ethylene, ethane, H ₂ , CO	Modified electrodes: 10 % methane and 33 % ethylene at -1.9
28	25	1	Cation ex. membrane	Cu mesh/foil	Pt mesh	CO ₂ , KHCO ₃	Aq. KHCO ₃	Ag/AgCl	Methane, ethylene, ethane, H ₂ , CO	Cu mesh: 15 % methane and 8 % ethylene at -1.9
29	-30	---	Nafion [®] 117	Cu foil	Pt foil	CO ₂ , sodium salts in methanol	KOH in methanol	Ag/AgCl	Methane, ethylene, formic acid, CO, H ₂	70.5 % FE methane in NaClO ₄ /methanol at -3V and 22.7 mA/cm ²
30	---	1 to 60	Nafion [®] 117	Cu wire	Pt plate	CO ₂ , LiClO ₄ in methanol	Aq. H ₂ SO ₄	Pb(Hg)x/PbSO ₄ /SO ₄ ²⁻	Methane, ethylene, CO, formic acid, acetic acid	FE At 20 bar: 25.5 % methane, 15.1 % CO, 22.1 % formic acid, 40.2 % acetic acid at -3V vs. Pb(Hg)x/PbSO ₄ /SO ₄ ²⁻
31	-30	---	Nafion [®] 117	Cu foil	Pt foil	CO ₂ , LiOH in methanol	KOH in methanol	Ag/AgCl	Methane, ethylene, CO, formic acid	78 % methane and ethylene at -4V

32	---	---	Selemion™ (cation)	Cu mesh/Cu-halide electrode	Pt plate	CO ₂ , potassium halides	Aq. potassium halides	Ag/AgCl	Methane, ethylene, ethane, CO, ethanol, H ₂	FE: CuBr electrode and KBr electrolyte: 5.8 % methane and 79.5 % ethylene at -2.4 V
33	---	---	FAB (anion) or no membrane	Pt/Nb plate (95% Pt)	Pt/Nb plate (95% Pt)	CO ₂ , methanol + [bmim][Br] + CH ₃ OK	Methanol + [bmim][Br] + CH ₃ OK	Ag/AgCl	Dimethyl carbonate	FAB membrane: 9.74 mmol/L, undivided cell: 80.85 mmol/L
34	25	1	Nafion®	Sn-GDE	Pt plate	CO ₂ , KHCO ₃	Aq. KHCO ₃	Hg/HgO, KHCO ₃	Formate, H ₂ , CO, methane traces	93 % FE formate at 50 mA/cm ²
35	25	1	Nafion® 117	Sn-GDE	DSA	CO ₂ , KCl + KHCO ₃	Aq. KOH	Ag/AgCl	Formate	Formate FE about 70 % and a concentration of 1348 mg/L
36	25	---	Nafion® 117	Sn-GDE	Pt foil	CO ₂ , KHCO ₃	Water	Ag/AgCl	Formate	FE 78 % formate at -1.8 V. 0.5 M KHCO ₃ used
37	---	---	Selemion™ (cation)	Net Ag-electrode	Pt plate	CO ₂ , KCl	Aq. KCl	Ag/AgCl	CO, H ₂	CO conversion 100 % (AgNO ₃ into the electrolyte). FE > 45% CO.
38	25	---	Nafion®	Sn-GDE + PTFE	Pt foil	CO ₂ , KHCO ₃	Aq. KHCO ₃	Ag/AgCl	Formate	FE 87 % formate at -1.8 V and 22 mA/cm ²
39	25	1	Nafion® 117	Cu ₂ O and Cu ₂ O/ZnO electrodes	Platinised titanium	CO ₂ , KHCO ₃	Aq. KHCO ₃	Ag/AgCl	Methanol	FE Cu ₂ O: 45.7 % at -1.3 V; FE Cu ₂ O/ZnO: 17.7 % at -1.3 V
40	25	1	Polymer electrolyte membrane	Pt-Glassy carbon electrode	Pt wire	Deionized water or KHCO ₃	Pure deionized water	Ag/AgCl	Formic acid	0 to 35 mM in continuous mode vs. 0 to 18 mM in discontinuous mode
41	25	---	Nafion® 117	Metal NP on carbon paper or CNT/GDL	Pt rod	CO ₂ , KHCO ₃	Aq. KHCO ₃	Ag/AgCl	Formic acid, acetic acid, methyl formate.	2.3e-4 M formic acid (Pt-CNT), 1.8e-4 M acetic acid (Pt-CNT), 1.7e-4 M methyl formate (Cu-CB)
42	22	---	Nafion® 117	Ag - Graphite GDL	Pt black NP	CO ₂ , [emim][Br]	Aq. H ₂ SO ₄	Ag/Ag+	CO, H ₂	FE > 9 % CO. 90% EE at 1.5 V
43	---	---	Nafion® 212	Ag NP	Pt NP	CO ₂ , EMIM-BF ₄	Aq. H ₂ SO ₄	SHE	CO	Rate CO ₂ conversion >> 5 nm Ag NP than Ag bulk electrode
44	---	---	Nafion® 117	Ag NP	Pt NP	CO ₂ , Aq. BMIM-BF ₄	Aq. H ₂ SO ₄	Ag/0.01 M Ag ⁺	CO	100 % FE to CO when 89.5 mol% water was added to the BMIM-BF ₄
49	---	---	Selemion™ (anion)	Cu: mesocrystals or NP or electropolished	Pt mesh	CO ₂ , KHCO ₃	Aq. KHCO ₃	Ag/AgCl	Formate, methane, ethylene, CO, H ₂	Cu mesocrystals: FE: 27.2 % ethylene, 17.5 % formate, 7.5 % CO, 2.7 % methane
56	25	1	Nafion® 961 and Nafion® 430	Pb plate	IrO ₂ /Ta ₂ O ₅	CO ₂ , K ₂ HPO ₄ + H ₃ PO ₄	Aq. KOH	---	Formate	FE 93 % formate at 2 mA/cm ² . Formate concentration increases with current density (higher value 0.01596 mol/L)
57	---	---	Nafion® 117	Cu mesh	Pt wire	CO ₂ , potassium halides	Aq. KHSO ₄	Ag/AgCl	---	CD excess: KCl < KBr < KI at -1,2 V
58	25	1	Nafion®	Cu rod. Electrocatalysts: Cu, CuO, ZnO, Mo ₂ C, Co ₃ O ₄	Pt/C (40% wt)	CO ₂ , KHCO ₃ or KOH or DMF	Water	---	---	Cu, CuO, ZnO, Co ₃ O ₄ activates catalysts in the protocol
59	10	---	Nafion® 112	Cu nanowires/nanonee	Pt foil	CO ₂ , KHCO ₃	Aq. KHCO ₃	RHE	Methane, ethylene, formic acid, H ₂	FE: Cu NNs: 14 % methane at -1.2V and 48 % formic acid at -0.9V; Cu NWS: 12 %

				dles						ethylene at -1.3V
60	19	---	Selemion™ (cation)	Different metal electrodes	---	CO ₂ , KHCO ₃	Aq. KHCO ₃	NHE	Methane, ethylene, CO, formate	FE in Cu electrode: 33.3 % methane and 25.5 % ethylene at -1.44V and 5 mA/cm ²
61	18	---	Cation ex. membrane	Cu single electrode/polycryst al Cu	---	CO ₂ , KHCO ₃	Aq. KHCO ₃	NHE	Methane, ethylene, CO, formate, H ₂ , alcohols	FE with Cu (110): 49.5 % methane y 15.1 % ethylene at -1.55V and 5 mA/cm ²

Table 2

Table 2. Experimental conditions, materials, main products and significant result of the Gas-Liquid electrochemical membrane reactors.

Ref.	T (°C)	Pressure (atm)	Membrane	Cathode	Anode	Catholyte	Anolyte	Reference electrode	Products	Main results
9	25	1	Nafion [®] / anion membrane	Ag	Pt-Ir (1:1) alloy	Humidified CO ₂ gas	Pure water/KH CO ₃	SCE	CO, H ₂	82 % FE CO with buffer layer and Nafion [®] membrane. 3 % FE CO with anionic membrane
41	25	---	Nafion [®] 117	Metal NP on carbon paper or CNT/GDL	Pt wire	CO ₂ gas	Aq. KCl	Ag/AgCl	CO, H ₂ , methanol, acetaldehyde, ethanol, acetone, isopropanol, acetic acid.	Best productivity to products: around 4.8e-4 mmol/h on Fe-CNT
45	25	1	Nafion [®] with buffer layer	Sn ink + GDL	Pt/C spray + GDL	CO ₂ gas	Aq. KOH	Ag/AgCl	Formate, CO, H ₂	70 % FE formate at -1.2 V
46	---	1	Anion electrolyte membrane	Silver-coated	Pt plate	CO ₂ gas	Aq. K ₂ SO ₄	SHE	CO, formic acid, H ₂	92.1 % FE CO at 20 mA/cm ² and 12.1 % formic acid at 100 mA/cm ²
47	22	---	Nafion [®] 115	Cu foil	Pt flag	Humidified CO ₂ gas	Aq. H ₂ SO ₄	SCE	Methane, ethylene	8 % FE methane and 10 % FE ethylene at -2 V
48	25	---	Nafion [®]	Cu-solid polymer electrolyte	Pt mesh	CO ₂ gas	Aq. K ₂ SO ₄	SCE	Methane, ethylene, CO, H ₂ , formic acid	FE > 89 % hydrogen
50	25	1	Nafion [®]	Carbon porous	Pt/C (40 % wt Pt)	CO ₂ gas	Alkali doped PVA	---	Formic acid, methanol, formaldehyde, CO, methane, H ₂	4.5 % FE to methane
51	---	---	Glass frit	Sn-GDL	Pt wire	CO ₂ gas	Aq. NaHCO ₃	Ag/AgCl	Formate	FE to formate: 70 % at -1.6 V vs. NHE
52	25	1	CMI-7000 or AMI-7001	Cu ₂ O on porous carbon paper	Pt/C (40% wt Pt)	Humidified CO ₂ gas	water	SHE	Methane, ethylene, methanol, H ₂	CMI-7000: FE > 80 % H ₂ ; AMI-7001: 30 % FE methane (2.5 V), 20 % FE methanol (2 V), 15 % FE ethylene (2 V)
53	25	1	PEI and QPEI doped with KOH (AEM)	Cu ₂ O on porous carbon paper	Pt/C	CO ₂ gas	Deionized water	---	CO, H ₂ , methane, ethylene, ethane	6-11 % FE CH ₄ at 2.75 V and 3-20 % FE C ₂ H ₆ at 2.25 V
66	60	---	Nafion [®]	TPE-CMP doped with Pt NP	Pt wire	CO ₂ gas	Aq. KHCO ₃	---	Hydrocarbons, hydrogen, CO, methanol, ethanol, isopropanol, acetic acid, acetaldehyde	Global FE > 95 %. Hydrocarbons and oxygenates: best results with Pt doped CNT and TPE-CMP
67	60	---	Nafion [®] 115	GDM-metal	Pt wire	50 % CO ₂ in He	Aq. KCl	Ag/AgCl	CO, H ₂ , hydrocarbons	18.9 % FE CO when Fe (metal doped) is used

				doped						
68	60	---	Nafion [®] 115	Pt or Fe doped TPE- CMP/CNTs	Pt wire	CO ₂ gas	Aq. KHCO ₃	Ag/AgCl	C1-C8 oxygenates.	Higher productivity with 70 % Pt/TPE-CMP + 30 % CNTs (7.2e-5 mmol/h).

Figure 1

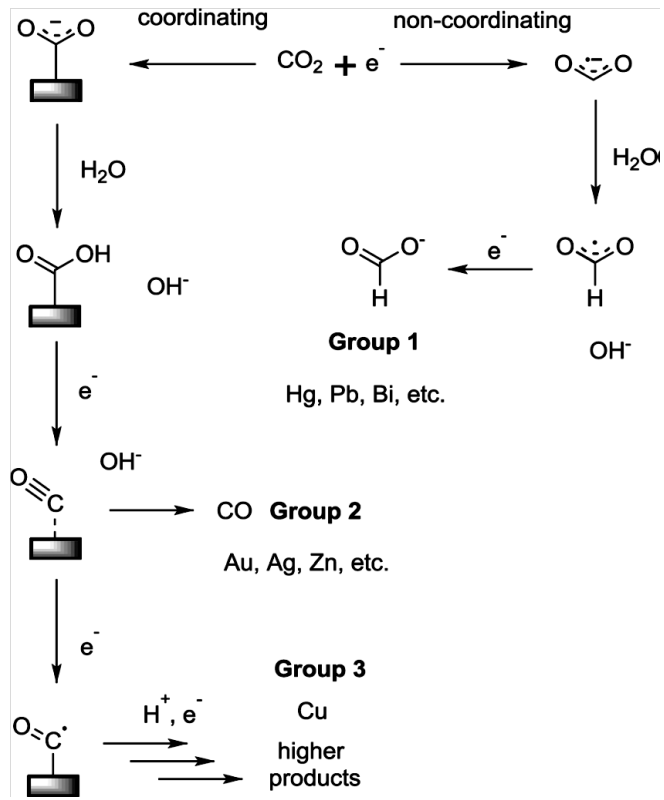


Figure 2

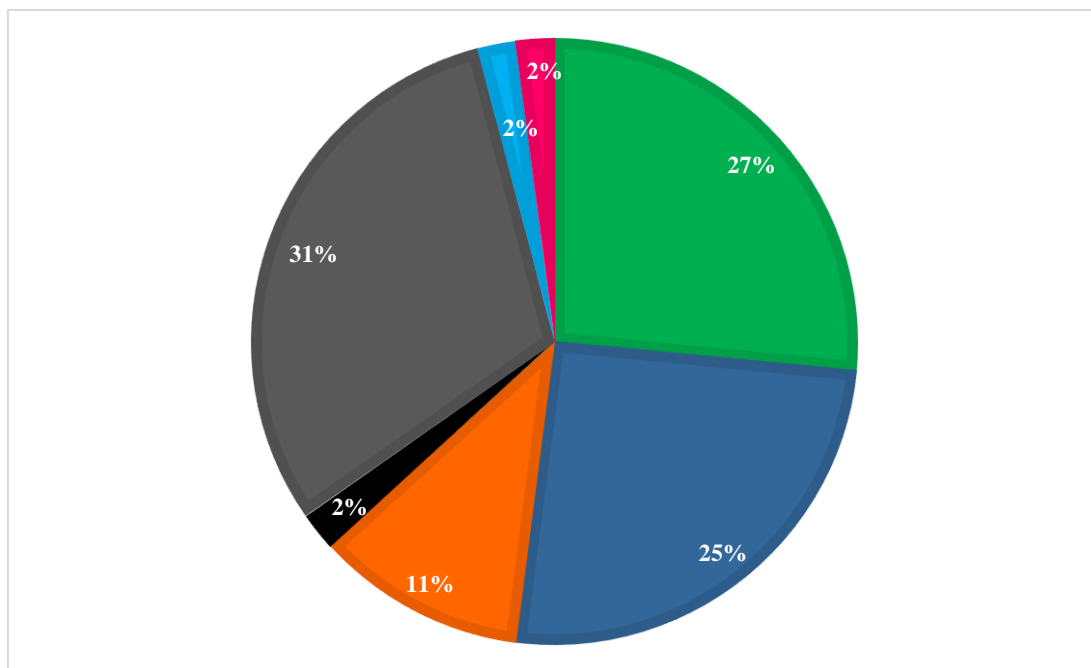


Figure 2. Distribution of the studies about ecMRs for CO₂ utilization by type of product.

Notation: formate; carbon monoxide; methane; ethylene; ethane; methanol; dimethyl carbonate.

Figure 3

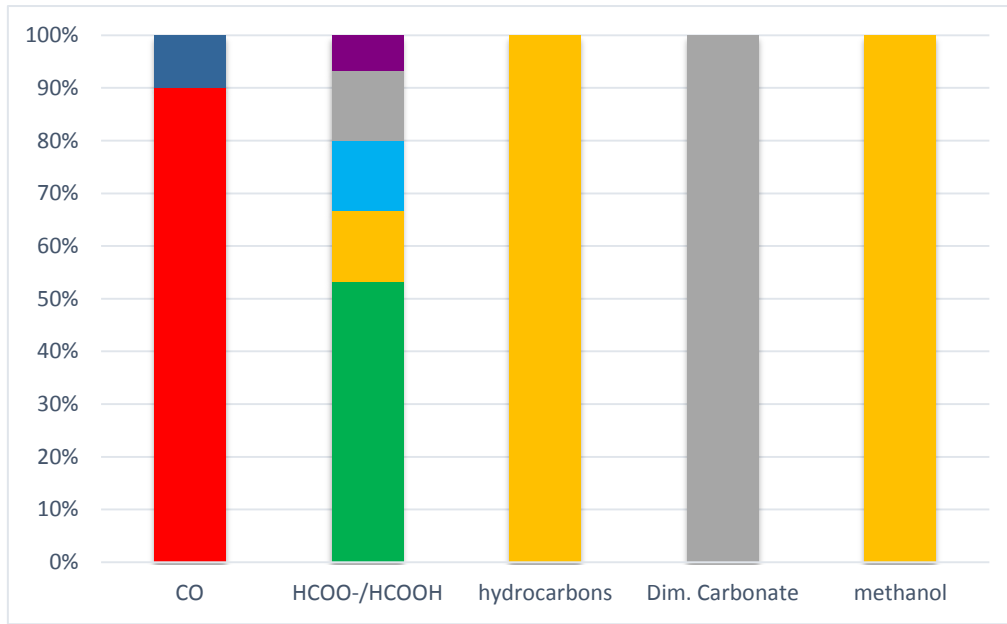


Figure 4

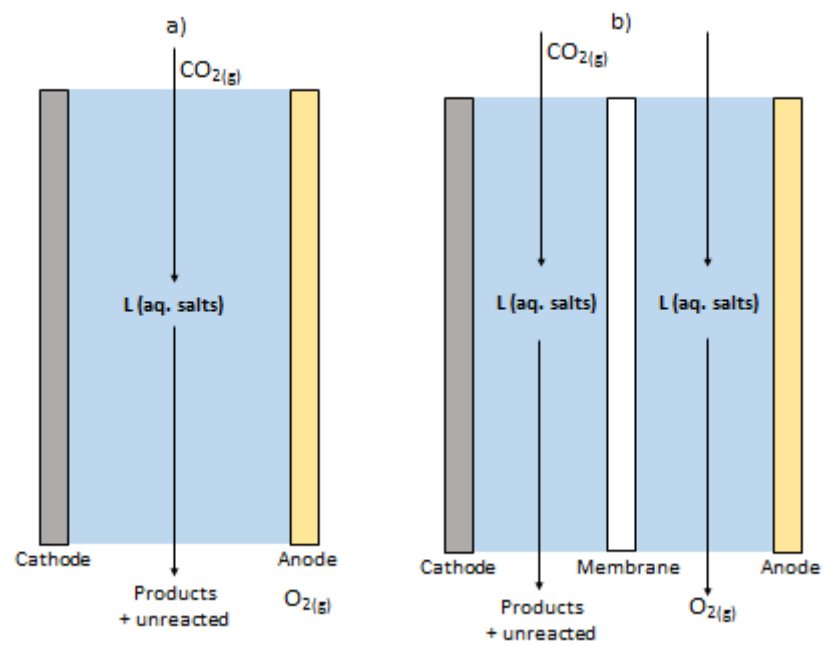


Figure 4. Conventional electrochemical reactor (a) and electrochemical reactor separated by an ion exchange membrane (b).

Figure 5

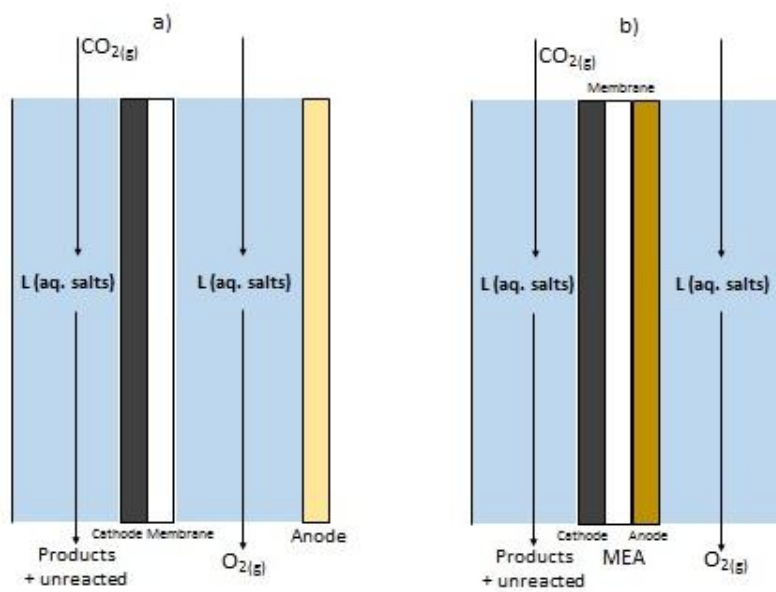


Figure 5. Catalysts dispersed at the cathode coupled with the membrane (a) and both electrodes coupled with the membrane (b).

Figure 6

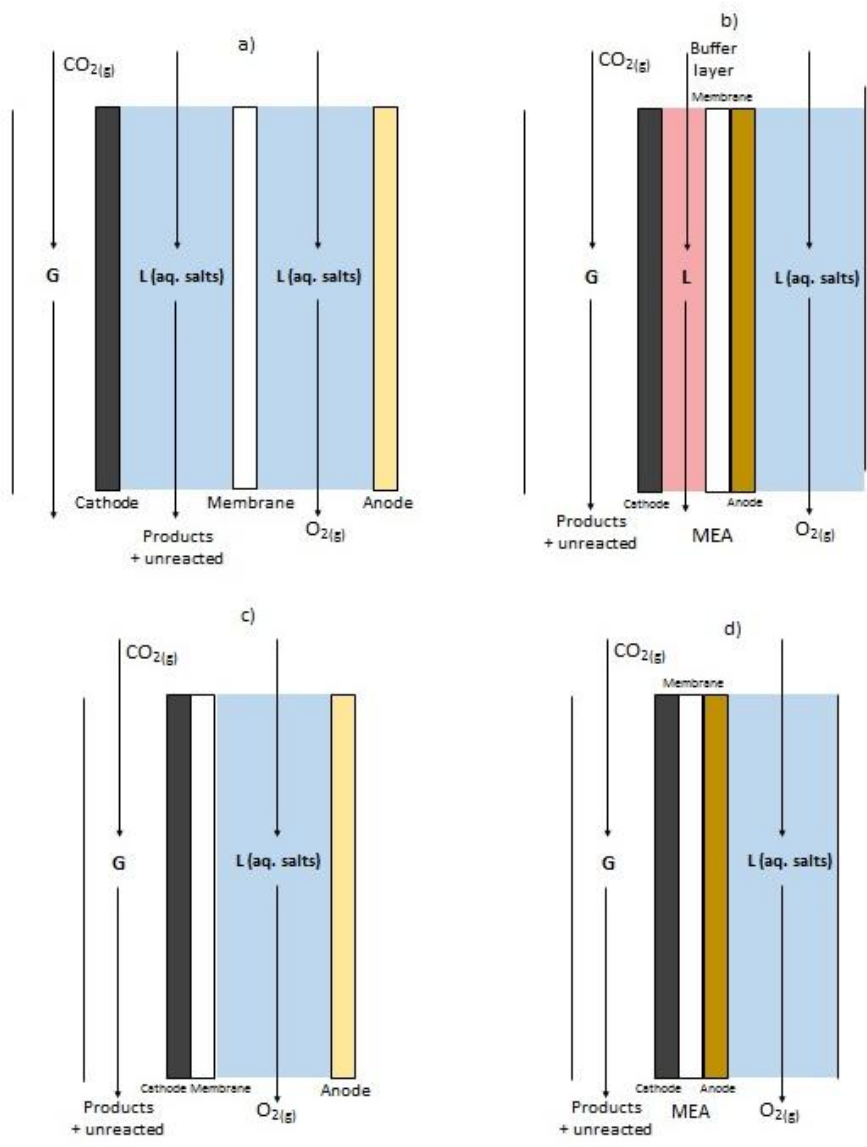


Figure 7

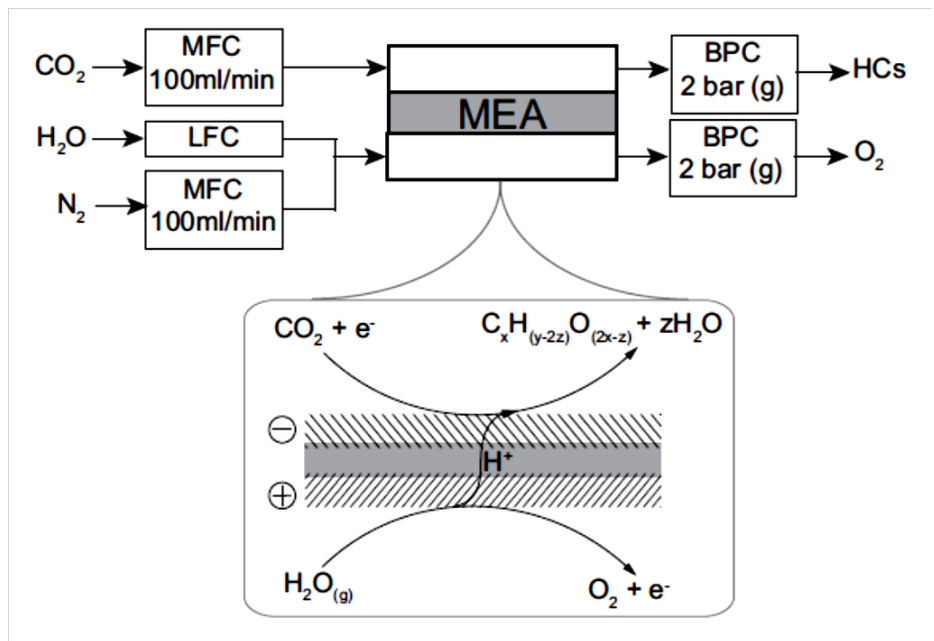


Figure 7. G-G ecMR used by Kriescher et al. [55]. Reproduced from Ref. [55].

Figure 8

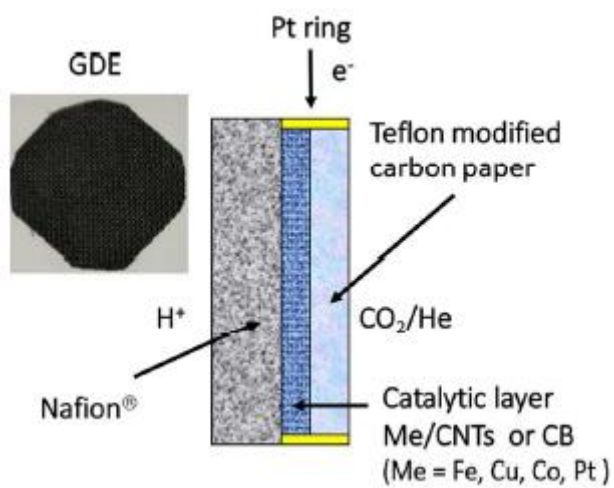


Figure 8. GDE type electrodes used for CO₂ electrochemical reduction. Reproduced from ref. [41]

Figure 9

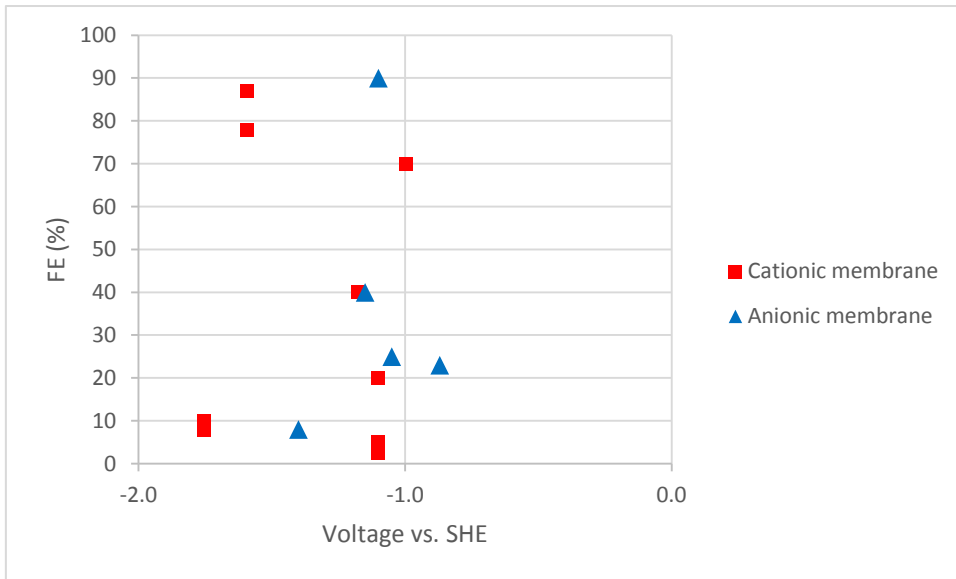


Figure 10

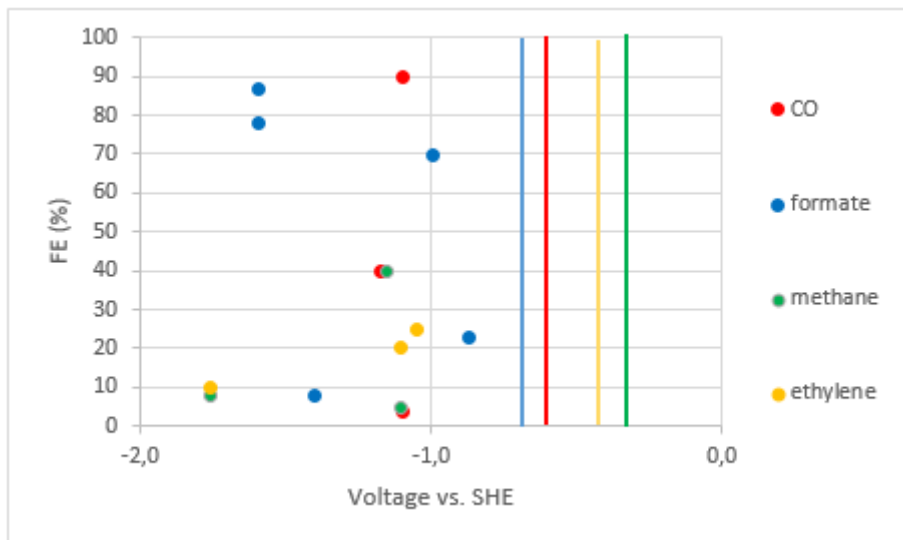


Figure 1. Mechanism for electrochemical CO₂ reduction on metal surfaces in water, reproduced from Ref. [7].

Figure 2. Distribution of the studies about ecMRs for CO₂ utilization by type of product.










Notation:  formate;  carbon monoxide;  methane;  ethylene;  ethane;  methanol;  dimethyl carbonate.

Figure 3. Different products as a function of the catalyst involved. Notation:  Ag; 

Ni;  Sn;  Pb;  Pt;  Cu.

Figure 4. Conventional electrochemical reactor (a) and electrochemical reactor separated by an ion exchange membrane (b).

Figure 5. Catalysts dispersed at the cathode coupled with the membrane (a) and both electrodes coupled with the membrane (b).

Figure 6. Gas phase used at the cathode separated to the catholyte (a), gas phase at the cathode with liquid buffer layer (b), cathode coupled to membrane without buffer layer (c), and both electrodes coupled to the membrane (d).

Figure 7. G-G ecMR used by Kriescher et al. [55]. Reproduced from Ref. [55].

Figure 8. GDE type electrodes used for CO₂ electrochemical reduction. Reproduced from ref. [41]

Figure 9. FE vs. voltage as a function of the membrane type used in L-L and G-L ecMRs.

Figure 10. FE vs. voltage as a function of valuable products obtained in L-L and G-L ecMRs. The points are experimental data and the lines are referred to the equilibrium potential for each product.

